

1 **Title:** Monoclonal antibodies targeting surface exposed epitopes of *Candida*
2 *albicans* cell wall proteins confer *in vivo* protection in an infection model

3 **Authors:** Soumya Palliyil^{1*}, Mark Mawer^{1,2}, Sami A Alawfi^{2†}, Lily Fogg^{1††}, Tyng H Tan^{1,2},
4 Giuseppe Buda De Cesare^{2†††}, Louise A Walker², Donna M MacCallum², Andrew J Porter¹,
5 Carol A Munro^{2*}

6 **Affiliations:**

7 ¹Scottish Biologics Facility, Institute of Medical Sciences, School of Medicine, Medical Sciences
8 and Nutrition, University of Aberdeen; Aberdeen, AB25 2ZP, United Kingdom

9 ²Aberdeen Fungal Group, Institute of Medical Sciences, School of Medicine, Medical Sciences
10 and Nutrition, University of Aberdeen; Aberdeen, AB25 2ZD, United Kingdom

11 †Present address: Taibah University; Medina, Kingdom of Saudi Arabia

12 ††Present address: Queensland Brain Institute, University of Queensland; Brisbane, 4072,
13 Australia

14 †††Present address: Department of Microbiology and Molecular Genetics, McGovern Medical
15 School, The University of Texas Health Science Center at Houston; Houston, Texas, USA

16 *Corresponding authors Email: soumya.palliyil@abdn.ac.uk ; c.a.munro@abdn.ac.uk

17 **Running title:** Anti-*Candida* cell wall protein human mAbs

18

19

20

21

22

23

24 **Abstract:**

25 MAb based immunotherapies targeting systemic and deep-seated fungal infections are still in
26 their early stages of development with currently no licensed antifungal mAbs available for
27 patients at risk. The cell wall glycoproteins of *Candida albicans* are of particular interest as
28 potential targets for therapeutic antibody generation due to their extracellular location and key
29 involvement in fungal pathogenesis. Here we describe the generation of recombinant human
30 antibodies specifically targeting two key cell wall proteins (CWPs) in *C. albicans* - Utr2 and
31 Pga31. These antibodies were isolated from a phage display antibody library using peptide
32 antigens representing the surface exposed regions of CWPs expressed at elevated levels during *in*
33 *vivo* infection. Reformatted human-mouse chimeric mAbs preferentially recognised *C. albicans*
34 hyphal forms compared to yeast cells and an increased binding was observed when the cells were
35 grown in the presence of the antifungal agent caspofungin. In J774.1 macrophage interaction
36 assays, mAb pre-treatment resulted in a faster engulfment of *C. albicans* cells suggesting a role
37 of the CWP antibodies as opsonising agents during phagocyte recruitment. Finally, in a series of
38 clinically predictive, mouse models of systemic candidiasis, our lead mAb achieved an improved
39 survival (83%) and several log reduction of fungal burden in the kidneys, similar to levels
40 achieved for the fungicidal drug caspofungin, and superior to any anti-*Candida* mAb therapeutic
41 efficacy reported to date.

42

43 **INTRODUCTION**

44 Invasive fungal infections (IFIs) are serious, life-threatening conditions typically affecting
45 individuals with a compromised immune system including patients with haematological
46 malignancies, those undergoing cytotoxic chemotherapy and organ transplantation (1).

47 Ironically, due to advancements in immunomodulatory drugs (including antibodies), patients
48 suffering from cancer and other complex health conditions are often left with a temporary but
49 weakened immune system due to their medication. This drug-induced immune suppression has
50 caused a significant rise in life-threatening systemic and organ specific fungal infections (1).
51 Clinicians suffer the frustration of successfully controlling cancers only to see their patients
52 succumb to these often hard to treat infections. Opportunistic pathogenic fungi, including
53 members of *Aspergillus*, *Candida* and *Cryptococcus* species, are responsible for invasive fungal
54 infections and the death of at least 1.7 million people each year globally (2). Population-based
55 surveillance studies show that the yearly incidence of invasive *Candida albicans* infections, and
56 related species including *Candida parapsilosis*, *Candida glabrata* and *Candida tropicalis*, can be
57 as high as 21 per 100,000 in some geographies (1). Furthermore, the ongoing global COVID-19
58 pandemic has fuelled an increase in secondary fungal superinfections, such as SARS-CoV-2
59 associated pulmonary aspergillosis (CAPA), with mortality rates greater than 40% in almost all
60 study cohorts (3).

61 Currently, IFIs are treated with antifungal agents belonging to four main drug classes, and
62 include amphotericin B, fluconazole, voriconazole, caspofungin and 5-flucytosine. The
63 recalcitrance of some infections has encouraged longer term treatment regimens and even their
64 prophylactic use for some surgeries and organ transplantation. This unmanaged use of a limited
65 drug armory has inevitably led to the emergence of antifungal drug resistance in many fungal
66 genera (4) (5). Certain *Candida* species, such as *Candida auris*, are of particular concern in
67 several countries with some isolates showing reduced susceptibility to fluconazole, amphotericin
68 B and echinocandins, with clinicians labelling *C. auris* the MRSA of the fungal world (6) (7).
69 The increasingly well-documented shortcomings of our existing antifungals (toxicity, complex

70 drug-drug interactions, emergence of multidrug resistance strains) and the intrinsic ability of
71 certain fungal species to evade drug therapies has accelerated the need to develop novel “first-in-
72 class” alternatives to tackle these life-threatening conditions.

73 In all pathogenic fungi of consequence, the cell wall is a dynamic structure continuously
74 changing in response to body/culture conditions and environmental stimuli. The cell wall of *C.*
75 *albicans* is covered in an outer layer of glycoproteins that play important roles in pathogenesis
76 and mediating interactions between the host and the fungus (8). These proteins “immune-mask”
77 fungal β -glucans from recognition by the mammalian β -glucan receptor dectin-1 (9). Some of
78 these cell surface glycoproteins, including adhesins, invasins and superoxide dismutases, are also
79 important virulence factors in their own right. Often shed by the invading fungus, these proteins
80 promote adherence of *C. albicans* to host cells, mediate tissue invasion and combat oxidative
81 burst defences (10). Many cell surface glycoproteins are post-translationally modified by the
82 addition of Glycosylphosphatidylinositol (GPI)-anchor and can be either fungal plasma
83 membrane localised or translocated into the cell wall, where they are covalently attached to the
84 β -(1,6)-glucan polymer (11). More than 100 putative GPI-anchored proteins have been
85 annotated in *C. albicans* using *in silico* analysis (12) (13), with some having enzymatic functions
86 associated with cell wall biosynthesis and cell wall remodeling. Several studies have reported
87 alterations in cell wall protein (CWP) composition and expression in response to changes in
88 growth conditions including carbon source, iron limitation, hypoxia or antifungal drug challenge,
89 indicating the possibility of up/down regulation of these proteins during *in vivo* infection (14).

90 Whilst CWPs define the success of many fungal pathogens, some may also provide an “Achilles’
91 heel” which can be exploited in therapy. Neutralising antibodies against CWPs have been
92 detected in patients’ sera and therefore represent an important source of antigens/epitopes for

93 vaccine generation and therapeutic antibody development (15). GPI-anchored CWPs, such as
94 Pga31 and Utr2, play important roles in cell wall integrity and assembly (16). Utr2 carries a
95 glycoside hydrolase family 16 domain, predictive of transglycosidase activity that catalyses
96 cross-links between β -(1,3)-glucan and chitin, as shown for the *S. cerevisiae* orthologue Crh1,
97 and is involved in cell wall remodelling and maintenance (17). In *C. albicans*, *UTR2*, *CRH11*,
98 and *CRH12* belong to the *CRH* gene family and are strongly regulated by calcineurin, a
99 serine/threonine protein phosphatase involved in cell wall morphogenesis and virulence (18)
100 (19). Mutants lacking *UTR2* exhibit defective cell wall organisation (inducing the cell integrity
101 MAP kinase signalling pathway), reduction in adherence to mammalian cells and reduced
102 virulence, resulting in the prolonged survival of animals in *in vivo* models of systemic infection
103 (18) (20). Immunofluorescence staining locates Utr2 predominantly to the budding site of
104 mother yeast cells, eventually forming a ring at the base of the neck, whereas during hyphal
105 elongation, the protein is detected at the tip of the germ tube and as a ring at the septum (18).
106 Utr2 co-localises to chitin-rich regions in yeast, pseudohyphal and hyphal forms (18).
107 Another GPI- anchored glycoprotein Pga31, which has unknown function, is upregulated in the
108 opaque form of *C. albicans* and after exposure to caspofungin (12) (21). A *pga31* null mutant
109 exhibits decreased chitin content compared to the wildtype strain and increased sensitivity to
110 caspofungin and cell wall perturbing agents such as Calcofluor white (CFW) and SDS (12). The
111 low chitin phenotype of the *pga31* null mutant points to a role for Pga31 linked to chitin
112 assembly during cell wall biogenesis and the maintenance of wall integrity under cellular stress.
113 Given their established roles in cell wall remodelling, upregulation after caspofungin treatment
114 (22) and enhanced expression in *in vivo* models of systemic candidiasis (23), we investigated the
115 potential of Utr2 and Pga31 as therapeutic targets for the development of monoclonal antibodies

116 (mAbs) to treat life-threatening fungal infections. MAb based therapies have seen
117 unprecedented levels of success in cancer and autoimmune disorders, producing several
118 blockbuster drugs including Humira®. This molecule class has also expanded into novel
119 therapeutic modalities such as bispecific antibodies and antibody-drug conjugates (ADCs) (24)
120 (25).

121 Cancer treatments were once dominated by toxic small molecule therapies requiring a balancing
122 act between killing the cancer cells and damaging healthy cells. However, cancer therapy was
123 revolutionised by targeted mAb therapies which have increased efficacy and reduced side-
124 effects. The balancing act is also practiced by infectious disease clinicians treating life-
125 threatening systemic fungal infections where toxic molecules are used to kill the fungus without
126 “killing” the patient. Unfortunately, mAb technology has failed to generate significant impact in
127 the infectious diseases field to date, but the increasing emergence of drug resistant fungal strains
128 is accelerating the need for new therapeutic modalities. Currently, only a handful of antifungal
129 mAbs are reported to show modest efficacy against *in vivo* infection and none of these have so
130 far progressed into the clinic (26) (27) (28)

131 In this study, the *C. albicans* cell wall proteome was interrogated using trypsin digestion
132 followed by LC-MS/MS analysis to identify several covalently linked CWPs, including Utr2,
133 Pga31, and their surface exposed epitopes. These epitopes were used to generate monoclonal
134 antibodies from a naïve human phage display antibody library. The ability of these recombinant
135 mAbs to bind several pathogenic fungi was investigated with some showing fungal-specific, and
136 others fungal species-specific binding. However, most importantly, their protective efficacy has
137 been demonstrated in a murine model of systemic candidiasis, with a potency approaching that
138 of more traditional antifungal drug classes.

139

140 RESULTS

141 Antigen design for recombinant antibody generation

142 Guided by the cell wall proteome analysis of various caspofungin susceptible and resistant
143 strains of *C. albicans*, peptide sequences accessible to trypsin digestion were identified and
144 matched with their respective fungal cell wall proteins (Tables 1A and 1B) (22). Based on the
145 predicted β turn structures (algorithm NetTurnP 1.0) and hydrophathy of these surface exposed
146 regions, peptide sequences were selected as antigens representing the CWPs Utr2 and Pga31. β
147 turn regions are often solvent exposed secondary structures and tend to have a relatively higher
148 propensity for antibody binding (29). A small panel of trypsin-susceptible peptides from both
149 proteins were custom synthesised and C terminally biotinylated via an additionally introduced
150 lysine residue and these conjugates used as antigens for biopanning experiments.

Utr2p peptides detected by LC-MS/MS	Pga31p peptides detected by LC-MS/MS
MSTFQESFDSK	HEGAALNYLFLAAPGVAENLK
IQFSLWPGGDSSNAK	QPLNVGNTVLQLGGSGDGTK
YGYYYAHIK	VDIAEDGTLSDGSDSVGAAK
EIYATAYDIPNDVK	NINDPYNYSK
GTIEWAGGLINWDSEDIKK	

151 **Table 1A. Amino acid sequences of the tryptic digested peptides identified in the cell wall**
152 **proteome analysis of *C. albicans* SC5314 using LC-MS/MS method.**

Associated Utr2 and Pga31 protein sequence as determined by the *Candida* Genome Database

<http://www.candidagenome.org/cgi-bin/protein/proteinPage.pl?dbid=CAL0000104>

<http://www.candidagenome.org/cgi-bin/protein/proteinPage.pl?dbid=CAL0004244>

Utr2p

MRFSTLHFAFLATLSSIFTVVAASDTTTCSSSKHCPEDKPCSQFGICGTGAYCLGGCDIRYSY
NLTACMPMPRMSTFQESFDSKDKVKEIELQSDYLGNSTEADWVYTGWVDYYDNSLLIQMP
NHTTGTVVSSTKYLWYGKVGATLKTSHDGGVVTAFILFSDVQDEIDYEFVGYNLNTPQSNY
YSQGILNYNNSRNSSVNNTFEYYHNYEMDWTEDKIEWYIDGKVRTLNKNDTWNETSRY
DYPQTPSRIQFSLWPGGDSSNAKGTIEWAGGLINWDEDIKKYGYYYAHIKEIYATAAYDI
PNDVKLDGNSTKESDYHAFLYNSTDGDASNIMLTTKKTWLGSDDATGFDPQNDDDEDSSSNK
AQETTITSVSGSSTITSVKTDSTKKTANVPAQNTAAAQATAKSSTGTNTYDPSAGVGGFVQ
DSKSTDSGSSGSSSQGVANSLNESVISGIFASICLGILSFFM*

Pga31p

MKFHMLRQKKIFVLEYIYKPDISSFSGKYLFLFFLFQSHINQLFDYIYFIQKYLYIMKFLTA
ASLLTLSSSALAAIKDIQLYAQSSNNEVNDFGISSRHEGAALNYLFLAAPGVAENLKYDDET
KTVYTELKAGSSTVRQPLNVGNTVLQLGGSGDGTKVDIAEDGTLSEFDGSDSVGAANKIN
DPYNYSKDSYAVVKGGDGAIPKLVAKFTGDDKESASSSSSSAAPEPTASSEAPKETPVYSN
STVTLYTTYCPLSTTITLTVCSVDCTPTVIETSGSVTVSSVQVPSKTASSEAAPPKTTVDSVSKP
APSGKKPTAAVTSFEGAANALTGGSVIAIAVAAAIGLVF*

153 *Table 1B. Mapping of the tryptic peptides identified in the cell wall proteome analysis onto C.*
154 *albicans Utr2p and Pga31p sequences. Peptides are shown in bold within the amino acid*
155 *sequences of each protein. The chitin binding region of Utr2, identified using SMART tool*
156 *analysis software (<http://smart.embl-heidelberg.de>), is underlined.*

157

158 **Isolation of *C. albicans* CWP specific recombinant antibody fragments from a human**
159 **antibody library through biopanning**

160 Phage display technology was employed to isolate Utr2 and Pga31 peptide specific antibody
161 fragments from a human antibody library in single chain fragment variable (scFv) format.
162 Following three rounds of selection using decreasing concentrations of biotinylated peptide
163 antigen, two phage clones specific for the Pga31 peptide and 14 positive binders that recognised
164 the Utr2 peptide were isolated and their unique scFv genes confirmed by DNA sequencing.
165 These clones were reformatted into soluble single chain antibodies (scAbs) by cloning their
166 respective VH-linker-VL region into the bacterial expression vector pIMS147 (30) to facilitate
167 detection in biochemical assays and quantification of soluble expressed protein by *Escherichia*
168 *coli* TG1 cells.

169 ScAbs from Pga31 biopanning reacted specifically to their peptide antigen and *C. albicans* wild
170 type strain SC5314 hyphae (Fig. 1A & 1B) and bound total cell lysates of *C. albicans* SC3514
171 treated with or without 0.032 µg/ml caspofungin (Fig. 1C & 1D). An increase in scAb binding
172 signal was recorded when lysate was prepared from the cells treated with caspofungin (Fig. 1C &
173 1D). This reinforced the hypothesis that Pga31 is overexpressed when the cells are grown in
174 caspofungin, and that is involved in cell wall integrity (22). As a confirmatory control
175 experiment, the scAbs did not bind to a *pga31*Δ mutant strain treated with/without caspofungin
176 (Fig. 1E).

177

178

179

180

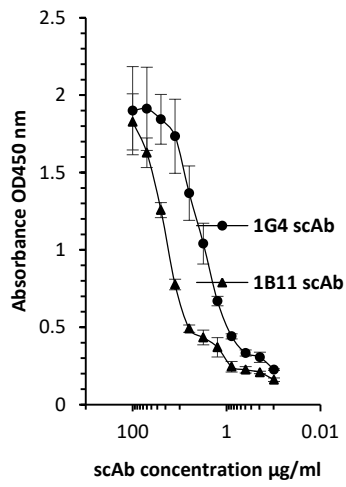
181

182

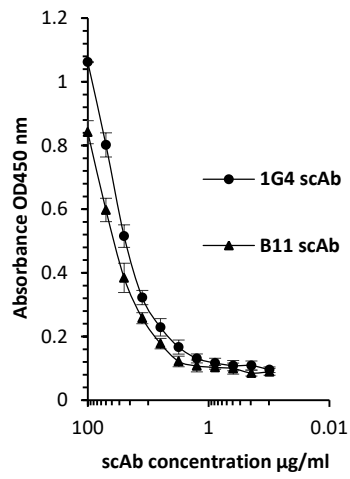
183

184

185 A

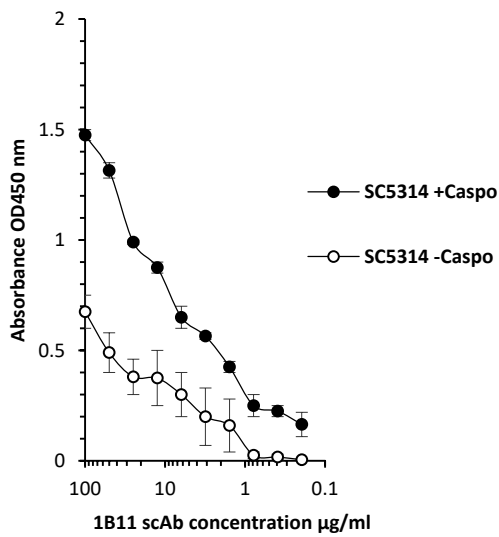


B

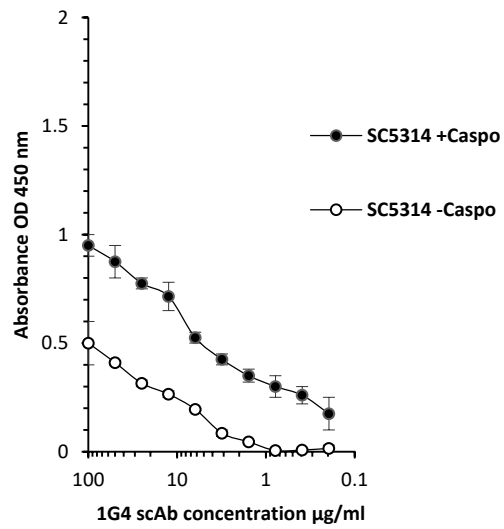


186

187 C



D



188

189

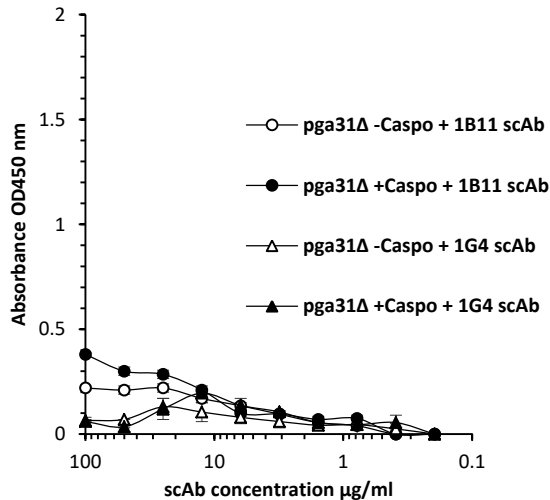
190

191

192

193

194 E



195

196 **Fig. 1. Pga31 scAbs binding profiles** (A) Antigen binding ELISA where wells are coated with
197 Pga31 peptide–biotin conjugate. (B) scAb binding to *C. albicans* SC5314 hyphae (C) scAb 1B11
198 binding to total cell lysate of *C. albicans* SC5314 treated with or without 0.032 µg/ml
199 caspofungin. (D) scAb 1G4 binding to total cell lysates of *C. albicans* SC5314 treated with or
200 without 0.032 µg/ml caspofungin. (E) Lack of binding for 1B11 and 1G4 scAbs to the cell lysates
201 of *C. albicans* pga31Δ mutant strain treated with or without 0.032 µg/ml caspofungin. Doubling
202 dilutions of scAbs were added to the plates coated with Pga31 peptide conjugate, *C. albicans*
203 SC5314 (-/+ caspofungin) or pga31Δ mutant (-/+ caspofungin) cell wall lysates and detected
204 using an anti-human C kappa HRP conjugated secondary antibody. Values represent the mean
205 absorbance OD450 nm readings (n=2, samples run in duplicate), error bars denote standard
206 error of the mean (SEM).

207

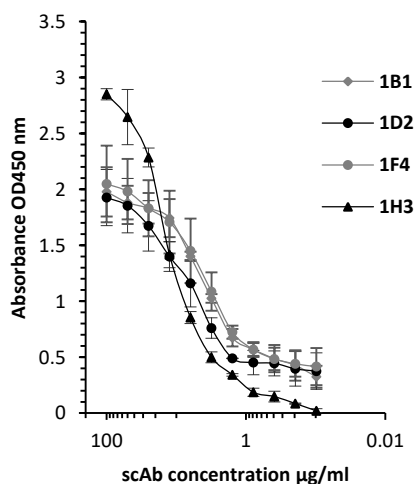
208 The antigen binding of top four Utr2 specific scAbs 1B1, 1D2, 1F4 and 1H3, selected based on
209 peptide-biotin conjugate ELISA signals, was confirmed (Fig. 2A) and these clones were tested
210 for their ability to recognise Utr2 in cell lysate preparations of *C. albicans* SC5314 yeasts (Fig.
211 2B). A non-specific negative control scAb was unable to bind to *C. albicans* cell lysate (Fig.
212 2B). The surface exposure and epitope accessibility of the Utr2 antigen peptide was established,
213 with all scAbs binding to *C. albicans* hyphal cells (Fig. 2C). When yeast cells were treated with
214 0.032 $\mu\text{g/ml}$ caspofungin, an increase in scAb binding was observed when compared to fungal
215 cells grown in the absence of the drug (Fig 2D-F). No scAb binding was seen when the *C.*
216 *albicans* single mutant strain *utr2* Δ and triple mutant strain *utr2* Δ :*crh11* Δ :*crh12* Δ were used
217 (Fig. 2G).

218

219

220

221 A

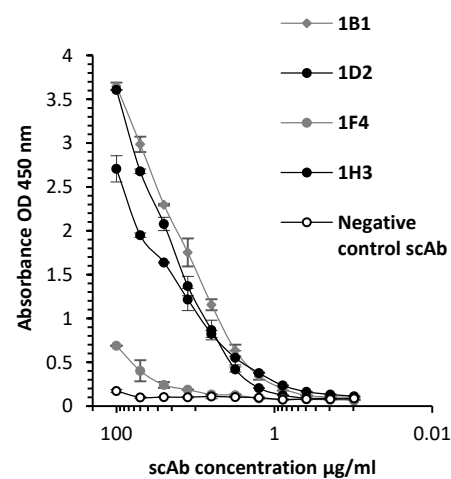


222

223

224

B

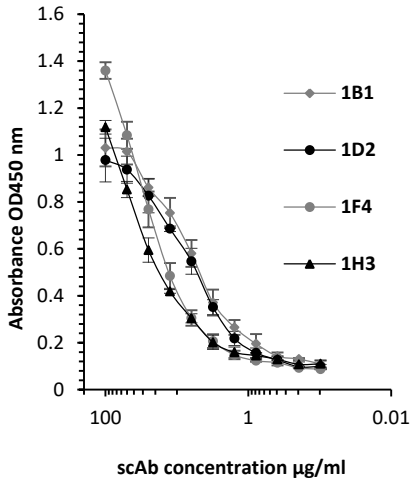


225

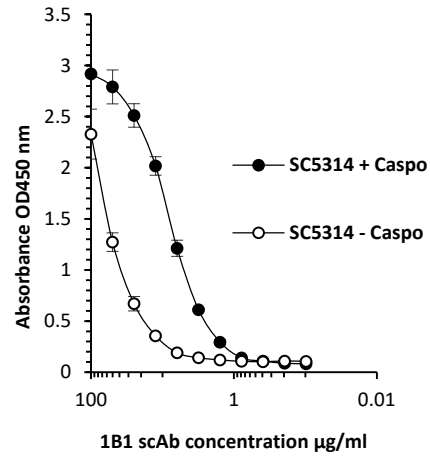
226

227

228 C

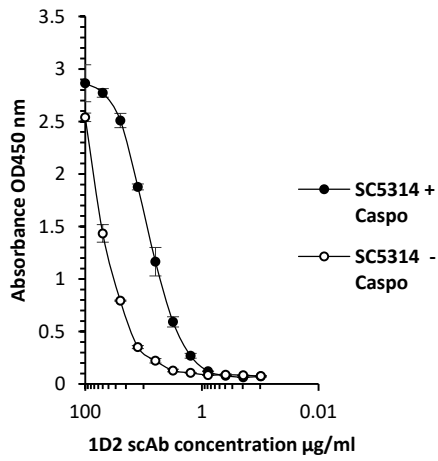


D

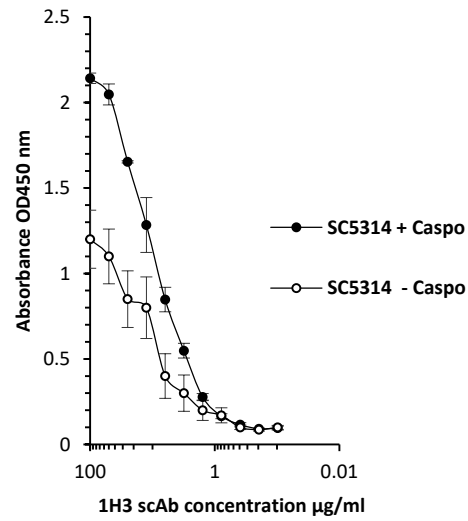


229

230 E



F



231

232

233

234

235

236

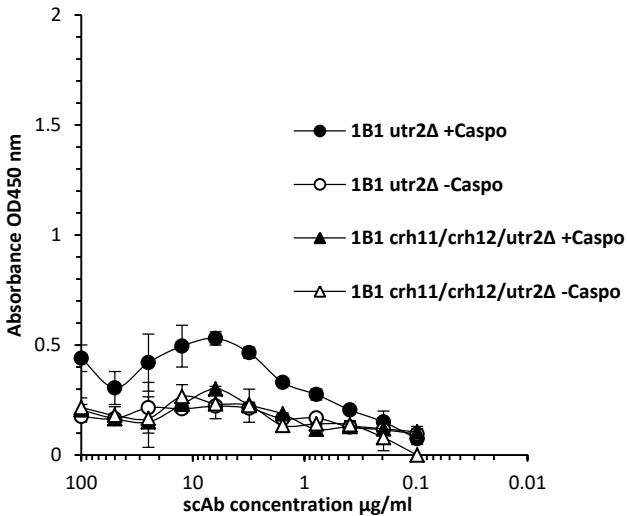
237

238

239

240

241 G



242

243 **Fig. 2. Utr2 scAb binding profiles** (A) Utr2 scAbs binding activity specific for the immobilised
244 Utr2 peptide, (B) scAb binding using a cell lysate preparation of *C. albicans* SC5314 (C) scAb
245 binding against *C. albicans* SC5314 hyphae (D-F) scAbs 1B1, 1D2 and 1H3 binding to *C.*
246 *albicans* SC5314 yeast cells treated with or without 0.032 µg/ml caspofungin. (G) Representative
247 scAb 1B1 binding to the cell lysates of a utr2 single mutant (utr2Δ) and triple mutant
248 (utr2Δ/crh11Δ/crh12Δ) treated +/- caspofungin at 0.032 µg/ml. ScAbs 1H3, 1D2 and 1F4 also
249 showed similar binding profiles with utr2Δ mutant strains, results not shown. Values represent
250 mean absorbance OD450 nm readings (n=2, samples run in duplicate) Error bars denote
251 standard error of the mean (SEM).

252

253 **Reformatting scAbs into human-mouse chimeric IgGs for *in vitro* and *in vivo* validation**
254 **studies.**

255 Utr2 scAbs 1D2, 1H3 and Pga31 scAb 1B11 were selected for IgG reformatting based on their
256 binding interactions with target peptides and *C. albicans* cells, and protein expression levels.
257 The VH and VL domain genes of the Utr2 scAbs 1D2, 1H3 and Pga31 scAb 1B11 were cloned
258 into a dual plasmid eukaryotic expression system encoding mouse IgG2a and kappa constant
259 domain genes and the resultant recombinant chimeric mAbs were expressed transiently in
260 HEK293-F cells. The presence of functional, protein A affinity-purified mAbs 1B11 and 1D2,
261 were confirmed by antigen binding ELISA with no cross-reactivity observed to unrelated peptide
262 sequences (Fig. 3A & 3B). MAb 1H3, which was selected against the Utr2 peptide, appeared to
263 also recognise a peptide sequence selected as a surface exposed region from the *C. albicans* cell
264 wall protein Phr2 (Fig. 3C). The reason for this is unclear.

265 The conversion of scAbs into a bivalent IgG format significantly increased (possibly in part *via*
266 avidity) the relative binding affinities of all three lead antibodies. Their EC₅₀ values (antibody
267 concentration required to achieve 50% reduction in maximum absorbance) were calculated by
268 extrapolating values obtained from direct antigen binding plots (Fig. 1A, 2A and 3A-C). The
269 calculated EC₅₀ for 1H3 scAb from the peptide binding assay was 175 nM, whereas the
270 reformatted 1H3 mAb achieved half maximal binding at 400 pM, an apparent 400-fold
271 improvement in functional affinity. Similarly, the EC₅₀ values obtained for 1D2 scAb and mAb
272 were 80 nM and 2 nM respectively. For the Pga31 clone 1B11, mAb reformatting resulted in
273 600-fold improvement in antigen binding compared to the parental scAb clone, with estimated
274 EC₅₀ values of 600 pM and 375 nM respectively.

275 In a whole cell binding ELISA, Pga31 mAb 1B11 preferentially recognise wild type *C. albicans*
276 (SC5314) hyphae compared to the yeast form (Fig. 3D), suggesting a morphology dependent
277 binding function which could signify increased epitope accessibility in this phenotype. Although

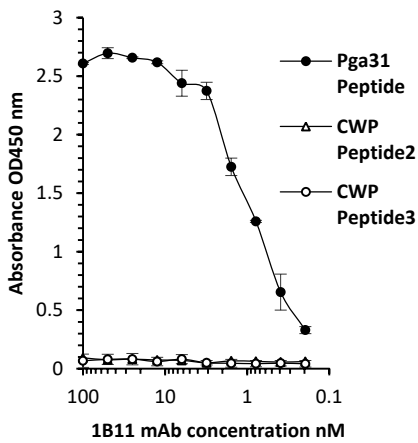
278 relatively poor binding activity was observed for the yeast form, when the cells were stressed
279 with caspofungin treatment, an enhancement in mAb targeting was seen (Fig. 3D). 1H3 and 1D2
280 mAbs were able to bind SC5314 cells immobilised on maxisorbant plates (Fig. 3E and 3F),
281 however similar to Pga31 mAb 1B11, Utr2 mAbs were also seen to display increased binding
282 activity for the hyphae when compared to the yeast cells.

283

284

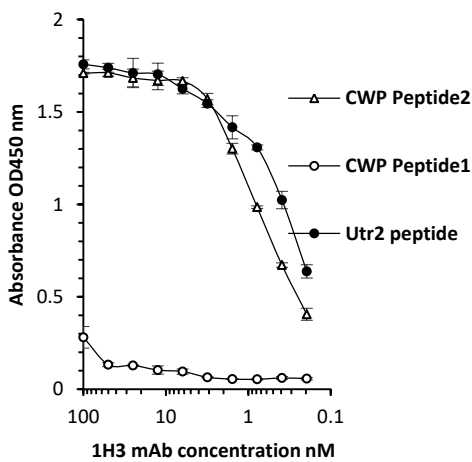
285

286 A



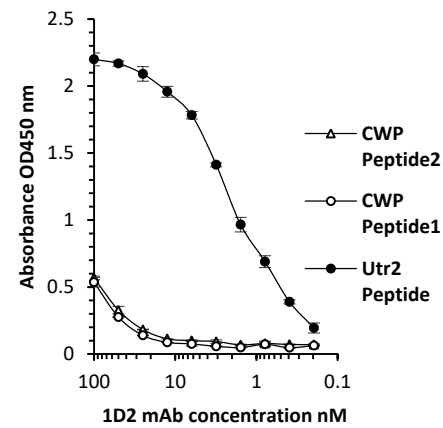
287

288 C

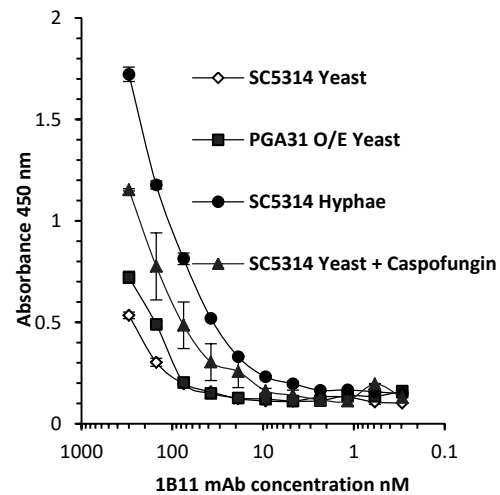


289

B

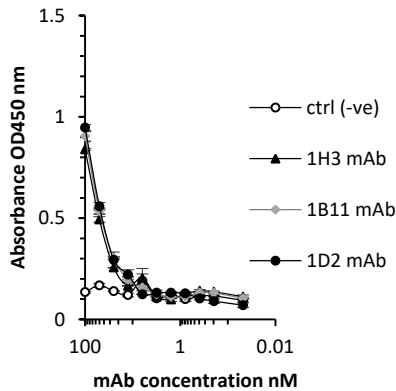


D

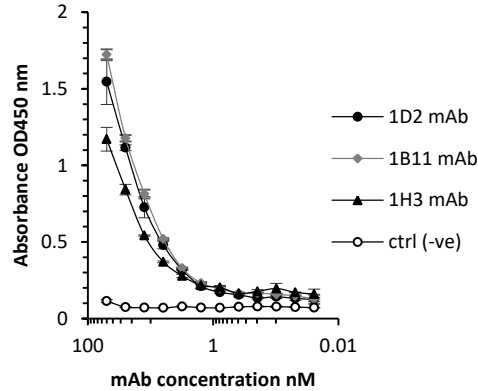


290
291
292
293
294

E



F



295
296

297 **Fig. 3. Reformatted Pga31 and Utr2 mAb binding profiles** (A) 1B11 mAb binding to
298 streptavidin captured biotinylated Pga31 peptide whilst assessing also the cross-reactivity for
299 other *C. albicans* cell wall proteins (CWP2 and CWP3) using peptide antigens isolated following
300 proteome analysis (B,C) 1D2 and 1H3 mAbs binding to streptavidin captured biotinylated Utr2
301 peptide and assessment of the cross-reactivity for other *C. albicans* cell wall protein peptide
302 antigens as above (D) 1B11 mAb binding to *C. albicans* SC5314 yeasts, a PGA31 over-
303 expressing strain, *C. albicans* SC5314 hyphae, and *C. albicans* SC5314 yeasts treated with 0.032
304 $\mu\text{g/ml}$ caspofungin (E) 1B11, 1H3 and 1D2 mAbs binding to *C. albicans* SC5314 yeast (F) 1B11,
305 1H3 and 1D2 mAbs binding to *C. albicans* SC5314 hyphae. The binding of mAbs to *C. albicans*
306 peptides and whole cells was detected and quantified using an anti-mouse IgG Fc region specific
307 HRP conjugated secondary antibody and the values plotted represent mean absorbance readings

308 at OD450 nm ($n=2$, samples run in duplicate). Error bars indicate standard error of the mean
309 (SEM)

310

311

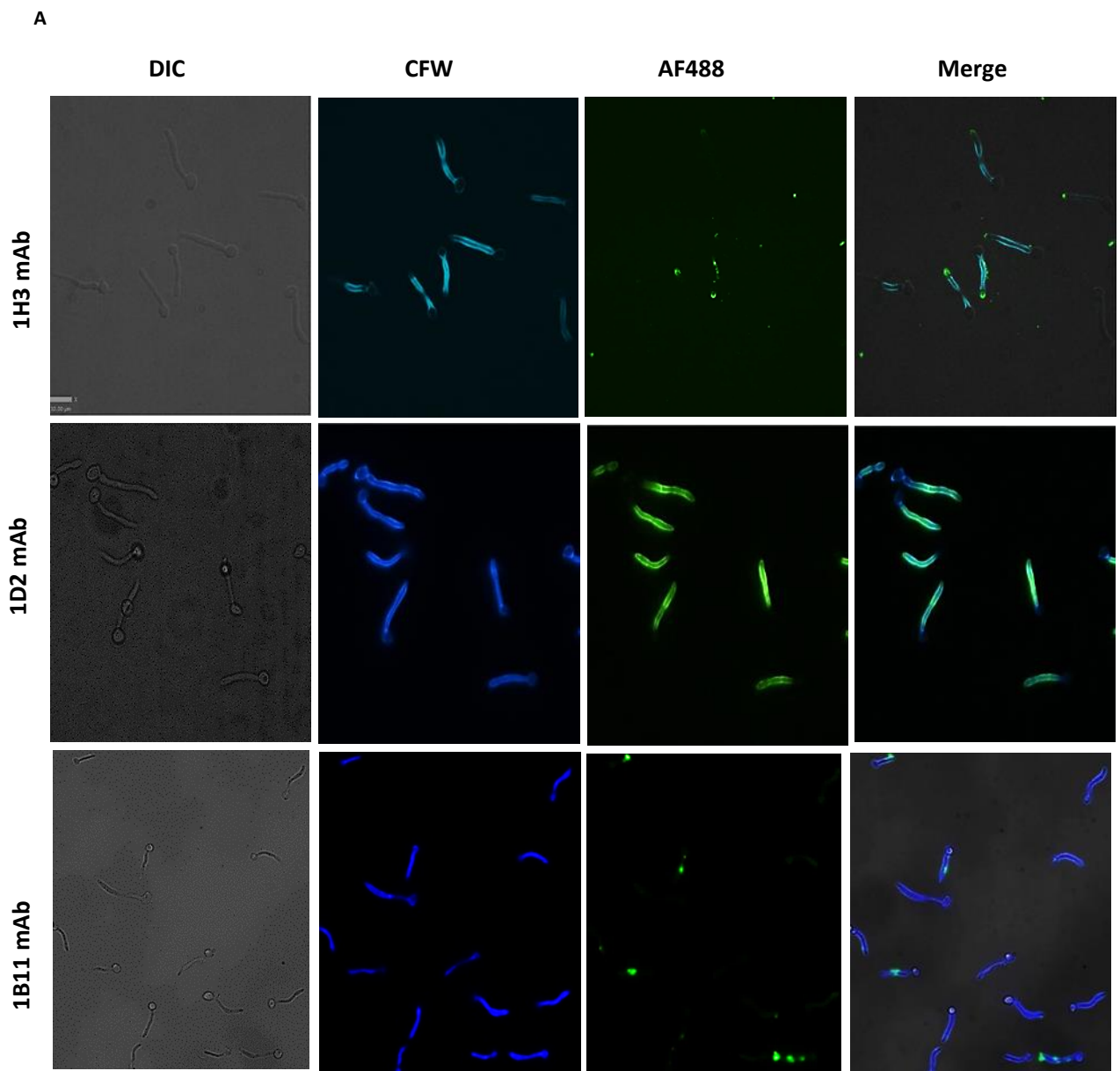
312 **Immunofluorescence staining of *C. albicans* using Utr2 and Pga31 antibodies**

313 Immunofluorescent microscopy using cell wall protein specific antibodies 1D2, 1H3 and 1B11
314 demonstrated specific and distinct binding patterns on *C. albicans* cells. Antibodies 1B11 (anti-
315 Pga31) and 1D2 (anti-Utr2) bound to *C. albicans* SC5314 hyphae but exhibited little or no
316 binding to mother yeast cells (Fig. 4). 1D2 staining was visible across the entire hyphal surface,
317 whereas 1B11 showed more punctate binding in distinct hyphal regions (Fig. 4A). The cross-
318 reactive 1H3 mAb (anti-Utr2), appeared to bind specifically to the apical tip of growing hyphae
319 (Fig 4A). When *C. albicans* SC5314 yeast cells were stained using anti-Utr2 and anti-Pga31
320 mAbs, a punctate binding pattern was observed on the surface of a limited number of cells (Fig.
321 4B). In contrast, when yeast cells were pre-treated with 0.032 $\mu\text{g/ml}$ caspofungin, strong
322 binding, again punctate in nature, was seen in a large proportion of cells at multiple sites
323 including regions of possible bud emergence (Fig 4C). Similar to hyphal staining, 1D2 mAb
324 produced a distinct binding pattern in budding yeasts, where staining was localised to the
325 emerging daughter cells in areas where new cell wall is being produced (Fig. 4C). The negative
326 control mAb did not show any staining of caspofungin treated or untreated cells (Fig. 4B). In
327 summary, all three antibodies displayed a morphology-specific binding pattern, including
328 increased binding to yeast cells treated with caspofungin, supporting the earlier ELISA data (Fig.
329 3).

330

331

332
333
334
335
336
337
338
339
340
341
342
343
344
345
346
347
348
349
350
351
352
353
354
355
356
357
358
359
360
361



362

363

364

365

366

367

368

369

370

371

372

373

374

375

376

377

378

379

380

381

382

383

384

B

DIC

CFW

AF488

Merge

1H3 mAb

SC5314 –

1H3 mAb

SC5314

1D2 mAb

SC5314 –

1D2 mAb

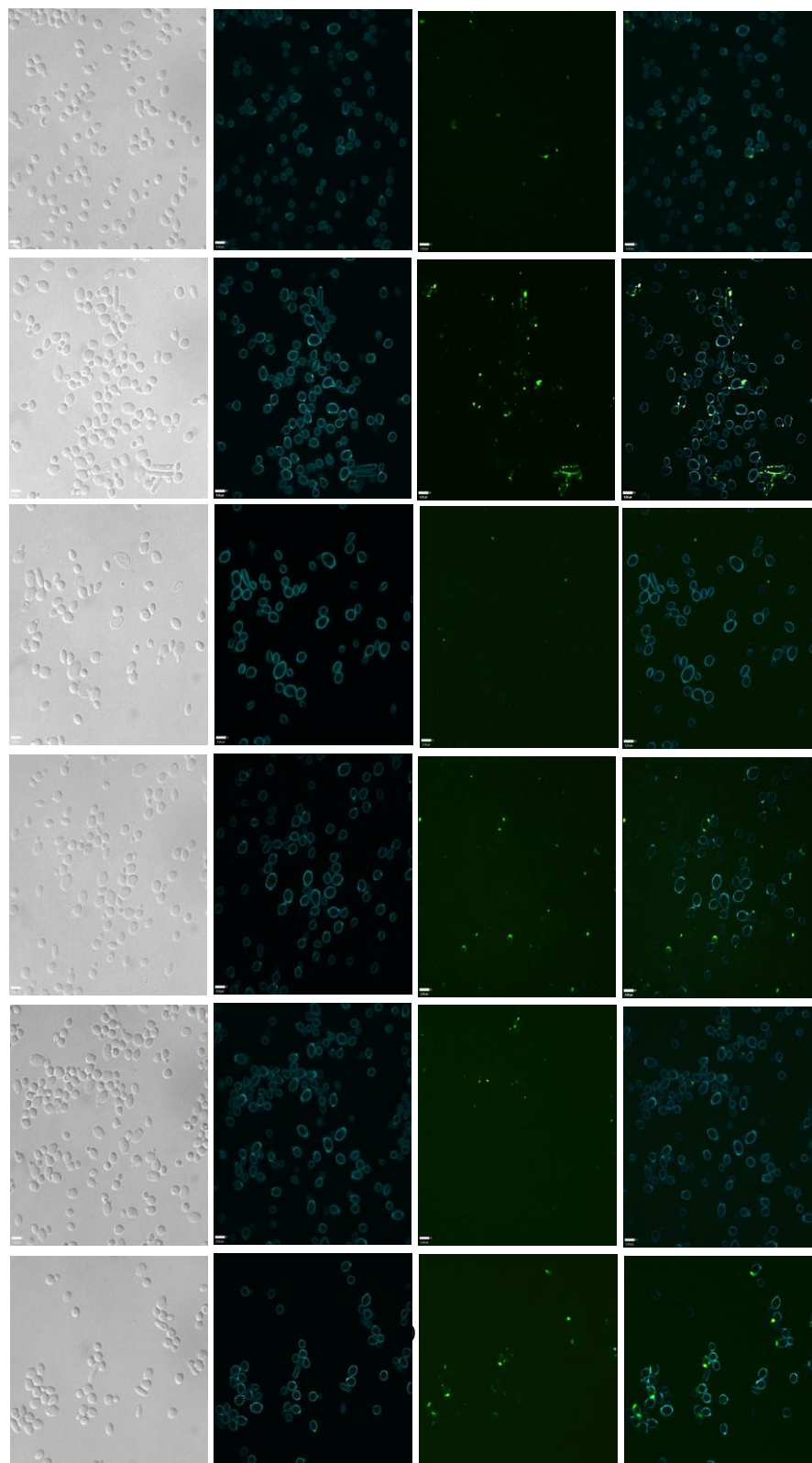
SC5314

1B11 mAb

SC5314 –

1B11 mAb

SC5314



385

386

387

388

389

390

391 **C**

392

393

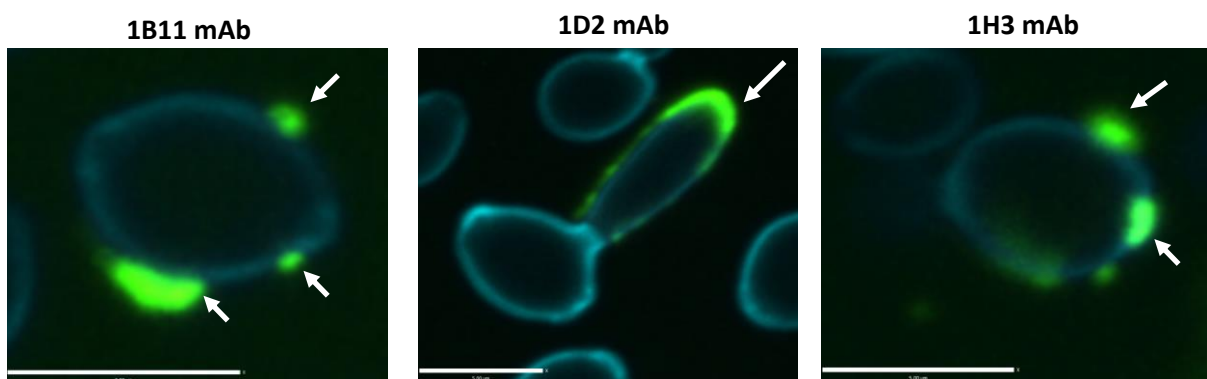
394

395

396

397

398



399 **Fig. 4. Utr2 and Pga31 antibody binding to C. albicans yeast and hyphae.** (A) *C. albicans*

400 *SC5314* hyphae immunostaining with 1H3, 1D2 or 1B11 antibodies. Calcofluor white (CFW)

401 was used to stain cell wall chitin and Alexa Fluor 488 (AF488) conjugated goat anti-mouse

402 IgG2a antibody was used to detect CWP-specific mAb binding. Green fluorescence indicates

403 antibody binding on the cell surface and distinct binding patterns were observed with the three

404 test mAbs. The anti-Utr2 antibody 1H3 binds at the apical tip of growing hyphae. In contrast,

405 the second Utr2 mAb 1D2 displayed uniform binding along the hypha. The anti-Pga31 mAb

406 1B11 had a more localised binding pattern with binding to a single major location on the

407 growing hypha.

408 (B) *C. albicans* SC5314 yeast cells treated with/without caspofungin (0.032 $\mu\text{g/ml}$) and
409 immunostained with 1H3, 1D2 or 1B11 antibodies or a negative control mouse Ig2a antibody.
410 Increased mAb binding was observed in caspofungin treated cells, mostly as a punctate binding
411 pattern around the poles of buds.

412 (C) The anti-Utr2 mAb 1D2 displays distinct binding, with intense staining localised around
413 zones of polarised growth and away from the mother cell. The second anti-Utr2 mAb 1H3 and
414 anti-Pga31 mAb 1B11 showed punctate binding on the cell surface (indicated by white arrows).

415

416 **Macrophage Interaction assay**

417 To evaluate the ability of CWP-specific mAbs to potentially confer protection in an infection
418 model, a macrophage interaction assay was performed using anti-Pga31 or anti-Utr2 mAbs as
419 opsonising agents for immune cell recruitment and mediation of phagocytosis. *C. albicans*
420 SC5314 untreated or pre-coated with test mAbs or a commercially sourced anti-*Candida* IgG
421 were used to challenge mouse J774.1 macrophage-like cells. The outcomes were visualised by
422 live cell video microscopy. Engulfment time (time taken for the macrophages to engulf *C.*
423 *albicans* cells) and the length of intracellular hyphae were determined.

424 Cells pre-incubated with mAbs and mouse IgG control were engulfed significantly more rapidly
425 when compared to *C. albicans* without antibody pre-treatment (Table 2). The vast majority
426 (95%) of fungal cells were engulfed within 7 min compared to 10 min for untreated cells
427 (Supplementary Fig. S1A-D). When incubated with anti-Pga31 or anti-Utr2 mAbs all fungal
428 cells were engulfed by 12 min; however, in the case of untreated *C. albicans*, this took 15 min
429 (Supplementary Fig S1A). These data suggest that anti-CWP mAbs influence macrophage
430 behaviour by targeting fungal cells for opsonophagocytosis.

Treatment group	Average engulfment time mean \pm SD (min)
SC5314 (wildtype)	5.64 \pm 2.59
SC5314+anti-Pga31 mAb	4.18 \pm 1.80
SC5314+anti-Utr2 mAb	4.28 \pm 1.96
SC5314+IgG positive control mAb	4.29 \pm 2.43

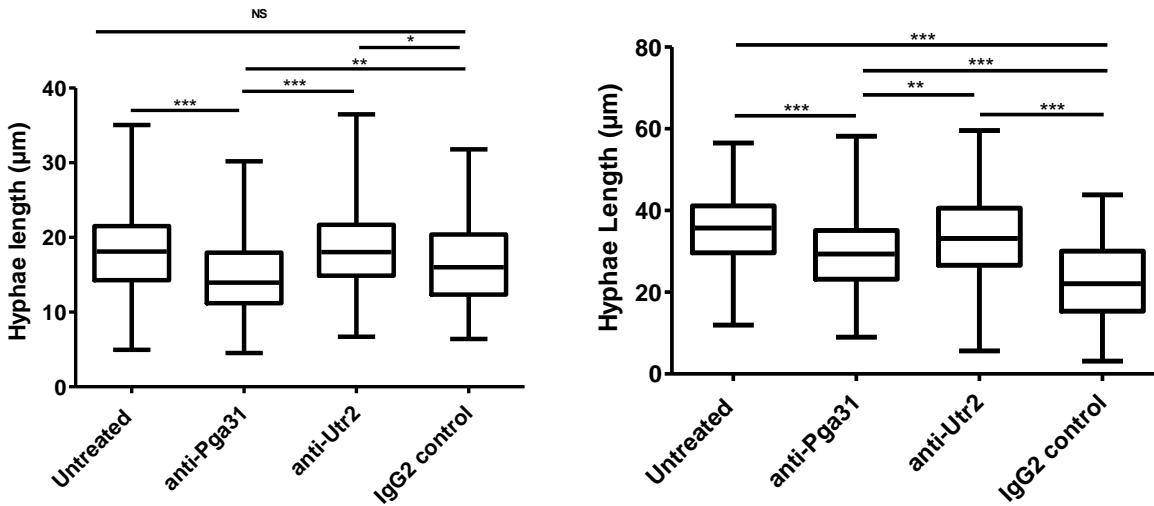
431 **Table 2. Time taken for J774.1 mouse macrophages to engulf anti-Candida mAb-treated or**
432 **untreated *C. albicans* SC5314. At least twenty-five macrophages were selected at random per**
433 **video to determine the engulfment time. Data represents average time taken \pm SD (min)**

434 The length of intracellular hyphae at multiple incubation times was also analysed from
435 microscopy videos (Fig. 5). Measurements were taken from the neck of the hypha to the apical
436 tip at 60 & 90 min following co-incubation with macrophages. Our data shows that intracellular
437 hyphae at 60 min were significantly shorter for *C. albicans* cells pre-incubated with anti-Pga31
438 mAb compared to all other treatment groups ($P = < 0.0001$) (Fig 5A). *C. albicans* cells pre-
439 treated with the positive control IgG were also shorter compared to untreated, but the difference
440 was only significant at 90 min (Fig. 5A & 5B).

441

442 A

B



443

444

445 **Fig. 5. Length of intracellular hyphae at 60 and 90 min.** Intracellular hyphal lengths were
446 measured (μm) following *C. albicans* uptake by J774.1 mouse macrophage at 60 (A) and 90 (B)
447 min. Twenty-five macrophages were selected at random per video to measure the length of
448 intracellular hyphae at two time points. Statistical significance was determined by Kruskal-
449 Wallis test with Dunn's multiple comparison test * $P < 0.05$, ** $P < 0.01$, *** $P < 0.005$.

450

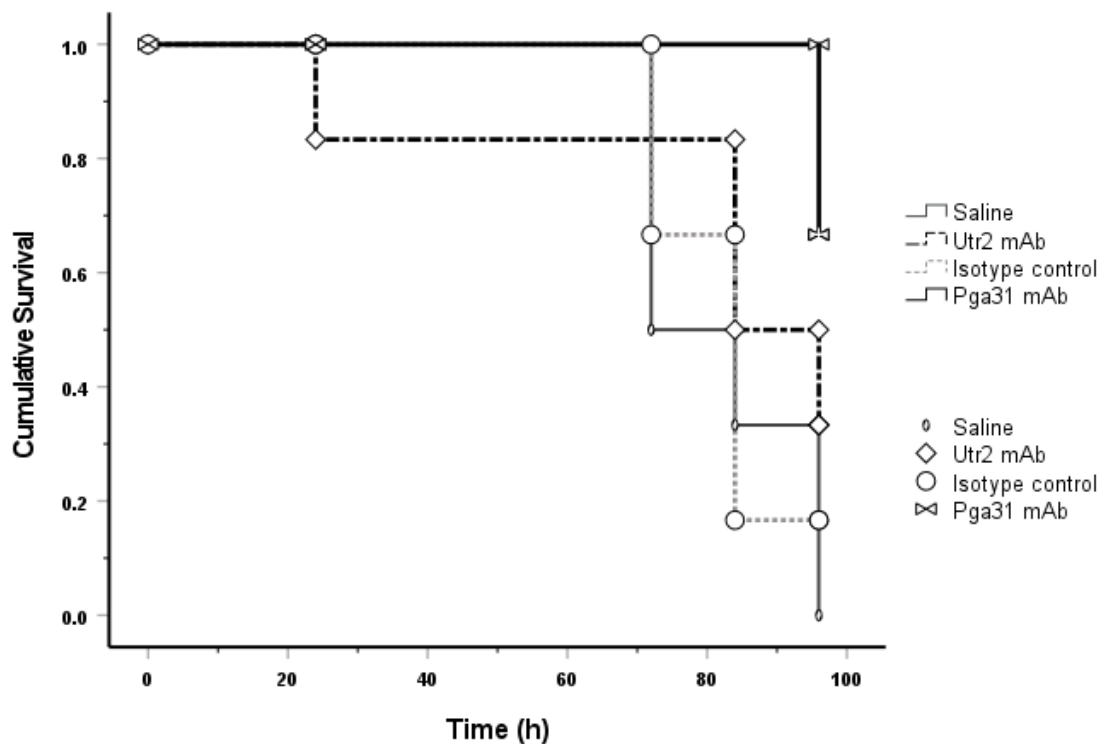
451 **Testing the therapeutic efficacy of anti-Utr2 and anti-Pga31 mAbs in a *C. albicans* mouse** 452 **infection model**

453 A series of *in vivo* mouse infection studies were conducted to evaluate the protective effect of
454 Pga31 and Utr2 mAbs in a disseminated candidiasis model, with the efficacy measured by
455 determining the organ fungal burden and mouse survival. In prophylactic study 1, mice were
456 pre-treated with 15 mg/kg of the test mAbs (including an isotype control), 3 h prior to IV
457 administration of *C. albicans* SC5314, followed by a second dose of mAb 24 h post-infection.
458 All treatments were administered intraperitoneally (IP) in 150 μl saline. In the anti-Pga31 mAb
459 treated group, 67% of mice survived four days post-infection, whereas the Utr2 mAb conferred

460 33% protection (Fig. 6A). Saline only and isotype control groups did not show any survival
461 benefit at 4 days. Comparing across all groups there were significant differences in survival
462 ($P=0.045$, Kaplan-Meier log-rank statistics).
463 Comparing the percentage weight change (day 0-2, supplementary Table S1) and kidney fungal
464 burdens (Fig. 6B), the differences were again statistically significant between some groups (P
465 <0.001 Kruskal-Wallis Dunn's multiple comparison test). In particular, when comparing the
466 fungal kidney burden of the saline only group to Pga31 mAb treated group ($P=0.004$) and weight
467 change ($P=0.011$). Utr2 treated group showed a significant difference for weight change only
468 ($P=0.023$). There was no difference in kidney fungal burdens between the isotype control IgG-
469 treated mice and saline-treated mice ($P>0.999$).

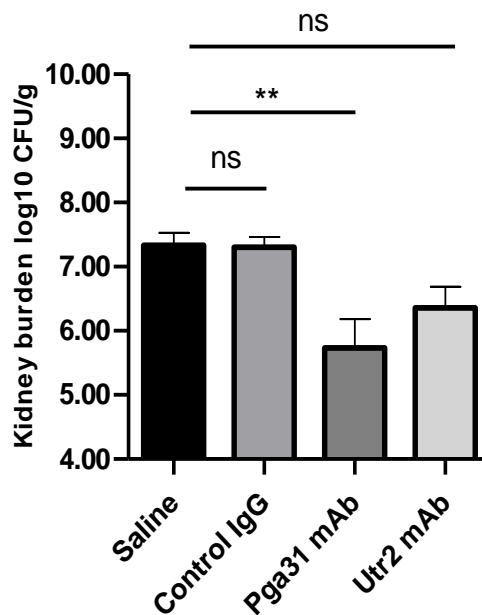
470

471



472

473 **Fig. 6(A).** *Kaplan-Meier survival curve representing the treatment effect of test mAbs and*
474 *control groups over 96 h in Study 1 Pga31 mAb 1B11 (15 mg/kg), Utr2 mAb 1D2 (15 mg/kg),*
475 *isotype control IgG (15 mg/kg) or saline were administered IP to mice 3 h pre and 24 h post-*
476 *infection with C. albicans SC5314. Mice (n=6/group) surviving the study period were treated as*
477 *censored data for analysis and statistical significance of survival between groups was*
478 *determined using the log-rank test.*
479



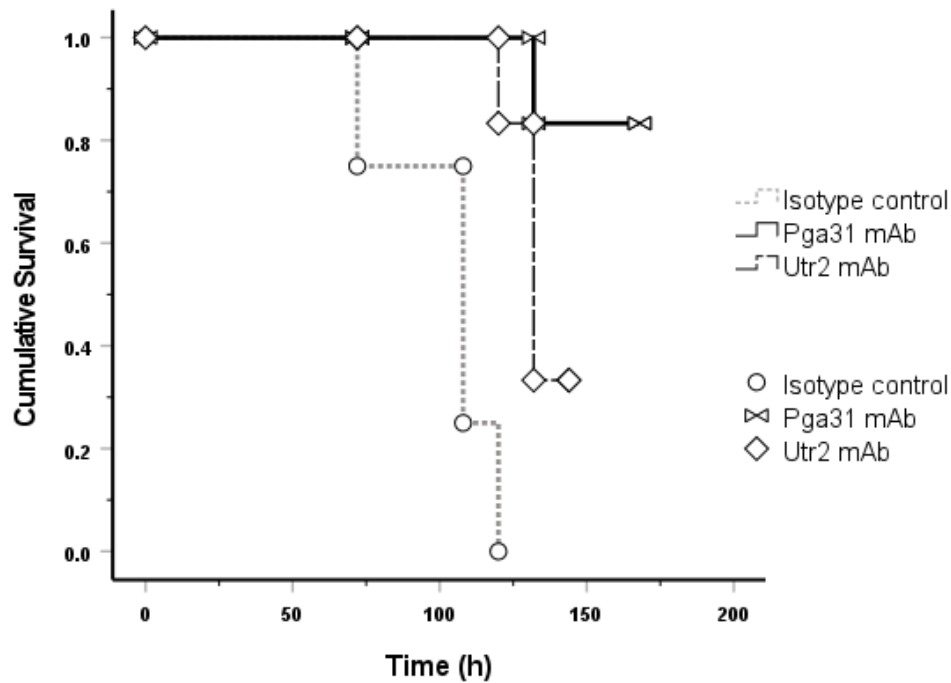
480
481
482
483
484 **Fig. 6(B).** *Mean fungal burdens in kidneys on day 4 post-infection in Study 1. Isotype control*
485 *IgG (15 mg/kg IP), Pga31 mAb 1B11 (15 mg/kg IP) and Utr2 mAb 1D2 (15 mg/kg IP) were*
486 *administered 3 h pre- and 24 h post-infection. Error bars denote standard deviation. A*

487 *significant difference was observed for kidney burden between the saline treatment group and*
488 *the 1B11 mAb therapy group (n= 6 mice/group; P=0.004, Kruskal-Wallis Dunn's multiple*
489 *comparison test)*

490

491 A second study was conducted to test the effectiveness of multiple dosing of antibodies. A
492 single 12.5 mg/kg dose was administered prophylactically followed by two treatment doses at 24
493 and 72 h post infection. All treatments were administered intraperitoneally (IP) in 150 μ l saline
494 and the survival of mice treated with Pga31 and Utr2 mAbs were compared with that of an
495 isotype control. Mice were monitored and weighed every day and were culled on day 6 post-
496 infection and fungal burdens in several organs including the kidneys, brain and spleen were
497 determined as before. While mouse survival of 83% was achieved with the Pga31 mAb
498 following a second dose 72 h post infection (vs 66.7% for study 1), no further improvement was
499 observed for the Utr2 mAb (33 % survival in study 1 and 2) (Fig. 7). Isotype control IgG
500 showed no therapeutic effect and the differences between various groups are statistically
501 significant ($P < 0.001$, log-rank test). A one log drop in kidney fungal burden, representing
502 killing of fungi or inhibition of cell division, for the Pga31 mAb treated group was achieved
503 when compared to the isotype control group (Pga31 mAb = 5.5. \log_{10} CFU/g vs isotype control =
504 6.8 \log_{10} CFU/g); however, there was little or no difference in mean fungal counts for the Utr2
505 mAb group (Utr2 mAb = 6.7 \log_{10} CFU/g vs isotype control = 6.8 \log_{10} CFU/g) (Table 3).
506 Similarly, fungal burden in associated organs including the brain and spleen was also reduced in
507 test antibody groups, with Pga31 mAb showing an improved therapeutic effect when compared
508 with the Utr2 mAb.

509



510

511

512 **Fig. 7. Kaplan-Meier survival curve representing the treatment effect of test mAbs and control**

513 **groups 6 days post-infection (Study 2). Pga31 mAb 1B11 (12.5 mg/kg), Utr2 mAb 1D2 (12.5**

514 **mg/kg) or isotype control IgG (12.5 mg/kg) were administered IP in mice 3 h pre and 24 h and**

515 **48 h post-infection with *C. albicans* SC5314. The difference between the three groups (n= 6**

516 **mice/group) is statistically highly significant ($P < 0.001$, Kaplan-Meier log-rank test)**

517

518

519

520

521

Mean \pm SD log₁₀ CFU/g of organs from
disseminated candidiasis model (n= 6)

	mice/group)		
	Kidney	Spleen	Brain
Isotype control	6.8 ± 0.7	4.0 ± 0.5	4.8 ± 0.4
Pga31 mAb	5.5 ± 0.5	3.3 ± 0.1	3.4 ± 0.7
Utr2 mAb	6.7 ± 0.7	3.6 ± 0.4	4.6 ± 1.0

522

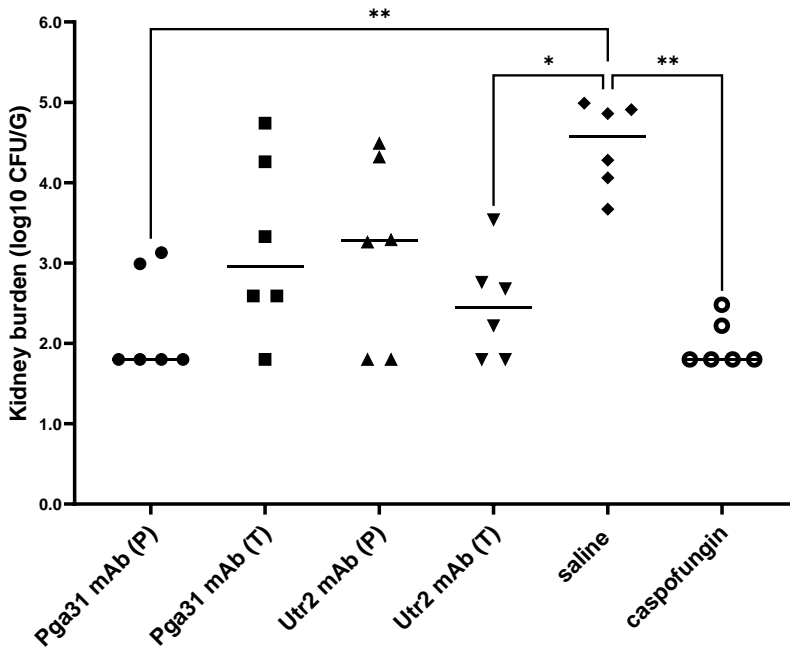
523 **Table 3. Mean fungal burdens in mouse organs at 6 days post-infection (Study 2). Control**
524 *IgG (12.5 mg/kg), Pga31 mAb 1B11 (12.5 mg/kg IP) and Utr2 mAb 1D2 (12.5 mg/kg IP) were*
525 *administered IP 3 h pre -infection and 24 h and 72 h post infection (n= 6 mice/group). Statistical*
526 *significance was achieved for fungal counts in the kidneys only (P=0.02, Kruskal-Wallis Dunn's*
527 *multiple comparison test).*

528

529 Finally, to compare the protective effect of test antibodies as a prophylactic agent vs treatment, a
530 follow-up study (Study 3) was conducted. In the prophylactic arm a single dose of each test
531 antibody was administered 3 h before infection followed by two doses at 24 h and 72 h post
532 infection. For the treatment only arm, mAbs were given 24 h and 72 h post infection and the
533 fungal burdens in the kidneys of various groups were compared with groups of mice receiving
534 saline or caspofungin (1 mg/kg) (Fig. 8). The Pga31 mAb prophylactic arm significantly
535 reduced the fungal burden in the kidneys of animals, 7 days post infection, which was similar to
536 the levels achieved with caspofungin treatment (Pga31 mAb = 2.22 log₁₀ CFU/g and caspofungin
537 = 1.98 log₁₀ CFU/g vs saline = 4.46 log₁₀ CFU/g, P=0.002, Kruskal-Wallis test). Mice receiving
538 only two doses of Pga31 mAb post-infection, also had reduced fungal burden in their kidneys
539 (3.22 log₁₀ CFU/g). Interestingly, for the Utr2 mAb groups, the treatment arm where the test
540 antibody was administered 24 h and 72 h post infection had reduced burden in the kidneys as

541 opposed to the prophylactic arm (Utr2 mAb treatment arm = 2.47 log₁₀ CFU/g vs prophylactic
542 arm = 3.16 log₁₀ CFU/g).

543



544

545 **Fig. 8. Kidney burdens at day 7 post-infection in prophylactic vs treatment study.** Test mAbs

546 (12.5 mg/kg per mouse) were administered 3 h pre-infection and/or 24 h and 72 h post-infection

547 (n= 6 mice/group). Pga31 mAb (P): prophylactic arm, antibody given pre- and post-infection,

548 Pga31 mAb (T): treatment arm, antibody given post-infection only, Utr2 mAb (P): prophylactic

549 arm, Utr2 mAb (T): treatment arm, saline only control, caspofungin at 1 mg/kg body weight

550 post-infection at 24 h and 72 h post-infection. Each symbol represents an individual mouse and

551 bar represents mean kidney burden in each group. The detection limit for kidney burden

552 determination was 2.3 log₁₀ CFU/g and therefore any samples with zero count were assigned a

553 value of one-half log below the detection limit (i.e. 1.8 log₁₀ CFU/g). Kidney burdens for the

554 different groups were compared by Kruskal-Wallis and Dunn's multiple comparison tests, *P <

555 0.05, **P < 0.01, ***P < 0.005.

556 **DISCUSSION**

557 With the advent of mAb technology, several groups have reported the development of protective
558 antibodies as a central part of a patient's recovery from infection (31). These mAbs typically
559 recognise antigens that are unique to the fungus and include fungal cell wall polysaccharides and
560 a small number of cell wall proteins (Als3, Sap2, Hsp90 and Hry1) involved in cell growth,
561 virulence and pathogenesis, as reviewed in (15) (32). Utr2 and Pga31 are CWPs covalently
562 linked to the fungal cell wall with their level of expression affected by carbon source (33) and to
563 infection-associated stress-conditions, including external stimuli such as challenge with
564 antifungal agents (34). We have recently reported an increased expression of Utr2 and Pga31
565 proteins, at proteomic levels, in *C. albicans* grown in the presence of caspofungin (22). In most
566 cases, the C terminal end of GPI-anchored proteins are buried inside the β -glucan skeletal layer
567 with only stretches of amino acids at the N terminal functional domain being surface exposed
568 (35). Surface epitopes of Utr2 and Pga31 were deduced from tryptic peptides generated from our
569 cell wall proteome studies and recombinant mAbs isolated that recognised CWPs in their native
570 conformation (Fig. 3D-F). Pga31 antibodies showed increased binding to *C. albicans* whole cell
571 lysates grown in the presence of caspofungin (Fig 1C-D), reaffirming observations that
572 antifungal agents alter CWP expression (22) and that Pga31 is expressed as a remodelling
573 mechanism for maintaining wall integrity under cellular stress. A role for Utr2 in establishing a
574 compensatory mechanism for the crosslinking of chitin and β 1-3 glucan in echinocandin-treated
575 cells has been reported previously (18). The abundance of Utr2 protein in the wall of
576 caspofungin-treated cells is confirmed here, with increased antibody binding to cell lysate
577 preparations (Fig. 2D-F). The target specificity of these antibodies was confirmed by a lack of

578 binding to mutant strains (*utr2* Δ and *utr2* Δ /*crh11* Δ /*crh12* Δ), even in the presence of caspofungin
579 (Fig. 2G).

580 We observed *C. albicans* cell morphology dependant immunoreactivity of CWP antibodies, with
581 preferential binding to the hyphal form when compared to yeast cells. Utr2 mAb 1D2 bound
582 uniformly along the growing hyphae, indicating broad surface exposure of this antibody's
583 preferred epitope. In contrast, the second Utr2 mAb 1H3, displayed a different binding pattern,
584 mostly localised to the apical tip of growing hyphae suggesting recognition of a second and
585 distinct epitope at the tip of the germ tube during hyphal elongation. The significance of the Crh
586 family of proteins including Utr2 in cell wall biogenesis and their temporal and spatial
587 organisation in various morphologies has been elegantly reported previously (18). This current
588 study supports the idea that Utr2 accumulation initially is localised to new budding sites in yeast
589 during the early growth phase, followed by re-localisation towards the base of the bud neck,
590 overlapping with the chitin ring later in the cell cycle. 1H3 and 1D2 mAb binding to cells pre-
591 treated with caspofungin also saw the greatest signal intensity at the new bud surface, further
592 supporting this finding.

593 Pga31 mAb binding resulted in a weaker but punctate signal in distinct hyphal regions of *C.*
594 *albicans* cells. This binding pattern is in agreement with previous reports and our own finding
595 that Pga31 is expressed at low or undetectable levels in *C. albicans* under normal laboratory
596 growth conditions. Pga31 is suggested to be part of the cell salvage pathway (16) and regulates
597 chitin assembly when cells are treated with cell wall perturbing agents, including calcofluor
598 white and caspofungin (12). In our study a marked increase in Pga31 binding was also observed
599 when cells were treated with caspofungin (Fig 4B).

600 The ability of J774.1 macrophages to engulf *C. albicans* cells treated with CWP specific mAbs
601 or an isotype control anti-*Candida* mAb was significantly higher than non-antibody treated cells
602 (Table 2). A complex interplay between macrophage and *C. albicans* has been previously
603 reported, with the pathogen sometimes counteracting the macrophage's defence strategies to
604 eventually break free and kill the macrophage as it escapes (36). In our study, whilst the
605 antibody mediated engulfment did not result in complete killing of *C. albicans*, a significant
606 inhibition of hyphal filamentation was observed which is tempting to speculate is due in part to
607 an immunomodulatory activity of mAbs involved in pathogen clearance. This was further
608 verified in a disseminated candidiasis mouse model, where protection from a life-threatening
609 infection was evident in animals receiving CWP-specific mAbs compared to an isotype control
610 mAb or vehicle alone. The Pga31 mAb, in particular, when administered as a single dose pre-
611 infection, followed by two doses at 24 h and 72 h post-infection, conferred improved survival
612 (compared to a single dose pre- and post-infection) of 83% vs 66%, respectively. The benefit of
613 double dosing was also reflected in the kidney fungal burdens with a very respectable three log
614 reduction (99.9%) in the number of fungal cells seen in the kidneys of mice receiving two doses
615 of mAb post-infection.

616 Other published *in vivo* efficacy models typically describe test mAbs that were either pre-
617 incubated with *C. albicans* cells or administered as a prophylactic pre-pathogen challenge, with
618 survival benefit and any reduction of fungal burden in associated organs reported (37) (27).
619 With these experimental design parameters, mAbs are already present in the systemic circulation
620 and able to bind to yeast cells, mediating opsonophagocytosis and clearance with enhanced
621 protection. Survival rates between 40% and 50% in a mouse model of systemic candidiasis have
622 been claimed for the β -(1 \rightarrow 3)-D-glucan mAbs (37) and, in a separate study, less than one log

623 reduction in kidney fungal burdens was reported for an anti-*C. albicans* mAb isolated from
624 patient B cells (27). Using a peptide biologic therapy, rather than a much larger antibody, a
625 small protective effect in animal studies with a one log drop in fungal burden was only seen in
626 “topical” vaginal and oropharyngeal candidiasis models (38). This less potent systemic efficacy
627 may be the result of the peptides “sticky” mode of action, low bioavailability or significantly
628 reduced half-life compared to mAbs (39) (40). Interestingly, in our study 3 design, CWP-
629 specific antibodies also reduced the fungal burdens in the kidneys of mice receiving treatment 24
630 h post infection, providing an early indication of their ability to bind *in vivo* to both yeast and
631 hyphal morphologies, possibly inhibiting cell replication and/or enhancing phagocytosis and
632 clearance. In the case of the anti-Utr2 mAb, double dose treatment did not translate into
633 increased survival compared to the single dose (33% in both study 1 and 2). But in study 3,
634 specifically investigating kidney fungal burdens, two doses of Utr2 mAb in the treatment only
635 group was more protective than mice receiving mAb as a prophylactic, followed by two doses
636 post infection. This data appears to reinforce our earlier observation that Utr2 mAb
637 preferentially binds to the hyphal form of *C. albicans* (Fig 4A).

638 With the serum half-lives of therapeutic human IgGs often reported in the region of 21-28 days
639 (a few days in mice) (41), immunotherapy for invasive fungal infections can reduce the dosing
640 frequency whilst addressing the serious drug resistance issues associated with long term
641 treatment regimens adopted in chronic infections. This is particularly pertinent for non-*albicans*
642 species including *Candida krusei*, *C. glabrata* and *C. auris* which are either intrinsically tolerant
643 or fully resistant to one or more class of existing antifungals, increasing the prevalence of non-
644 treatable nosocomial infections (42). Off-target toxicity and drug-drug interactions are other
645 important treatment considerations associated with existing antifungal therapies. Each drug class

646 has its own clinical challenges: nephrotoxicity of polyenes (43), amphotericin B interactions
647 with hypokalaemic drugs resulting in cardiac and skeletal muscle toxicity, and azole-mediated
648 inhibition of metabolising liver enzymes (e.g. cytochrome P450) leading to decreased catabolism
649 of co-administered drugs and dose related toxicities (44). It is widely recognised that targeted
650 biological agents, such as monoclonal antibodies, can overcome many of the toxicity and drug
651 resistance hurdles created by using small molecule drugs, with a handful of mAbs now approved
652 by the FDA as prophylactic treatments against bacterial and viral infections (45). One could
653 easily envisage scenarios where patients undergoing chemotherapy or organ transplant might
654 receive long-acting, antifungal mAbs as prophylaxis against life-threatening invasive fungal
655 infections prevalent in these immuno-compromised groups. These mAbs could be used as part
656 of a co-therapy regimen to augment or prolong the activity of existing, but limited in number,
657 systemic antifungals and address the issue of drug resistance, especially with fungistatic azole
658 compounds. By simultaneously targeting the pathogen with an antifungal agent and a mAb
659 adjuvant, the same level of efficacy can be achieved with lower drug doses, thereby significantly
660 improving the narrow therapeutic window associated with commonly used antifungals.

661 In this present study we successfully identified mAbs as lead molecules in a new antifungal drug
662 class as the first step in providing alternatives to our current and very limited antifungal drug
663 portfolio. A panel of recombinant, fully-human, monoclonal antibodies to surface exposed
664 epitopes of key fungal cell wall proteins in a range of fungal pathogens have been isolated and
665 characterised. These antibodies have been selected to recognise target proteins in their native
666 conformation and confer excellent levels of protection (over 80%) in a mouse model of
667 disseminated candidiasis, in part, through the recruitment of phagocytic macrophages via
668 antibody mediated opsonisation. These novel antifungal mAbs are now entering later-stage

669 preclinical evaluation to investigate additional aspects of their mode of action, levels of *in vivo*
 670 tolerability and pharmacological activities including PK/PD profiles, in relevant animal models.

671 MATERIALS AND METHODS

672 Fungal strains, media and growth conditions

673 All fungal strains used in this study are shown in Table 4 and were cultured from glycerol stocks
 674 (-70 °C) and maintained on YPD agar plates containing 2% (w/v) glucose, 2% (w/v) mycological
 675 peptone, 1% (w/v) yeast extract, and 2% (w/v) agar (all from Oxoid, Cambridge, UK). For *C.*
 676 *albicans* strains, unless stated otherwise, a single colony was grown in YPD medium (see above
 677 without the agar) and grown overnight at 30 °C with shaking at 200 rpm. To induce hyphal
 678 formation, cells were grown in RPMI-1640 modified medium (Sigma-Aldrich) containing 10%
 679 heat-inactivated foetal calf serum (FCS) and incubated at 37 °C for 2-4 h. For mouse studies, *C.*
 680 *albicans* SC5314 was grown in NGY medium containing 0.1% Neopeptone (BD, Wokingham,
 681 UK), 0.4% glucose, 0.1% yeast extract (BD) at 30 °C with constant rotation at 200 rpm.

Strain	Description	Genotype	Reference
SC5314	Clinical isolate	Wild-type	(46)
GPY03	<i>utr2</i> Δ	<i>ura3</i> Δ:: <i>λimm434</i> / <i>ura3</i> Δ:: <i>λimm434</i> , <i>utr2</i> Δ:: <i>hisG</i> / <i>utr2</i> Δ:: <i>hisG-URA3-hisG</i>	(18)
GPY102	<i>crh11</i> / <i>crh12</i> / <i>utr2</i> Δ	<i>ura3</i> Δ:: <i>λimm434</i> / <i>ura3</i> Δ:: <i>λimm434</i> , <i>utr2</i> Δ:: <i>hisG</i> / <i>utr2</i> Δ:: <i>hisG</i> ; <i>crh12</i> Δ:: <i>hisG</i> / <i>crh12</i> Δ : <i>hisG</i> ; <i>crh11</i> Δ:: <i>hisG</i> <i>crh11</i> Δ:: <i>hisG-URA3</i> - <i>hisG</i> ;	(18)
CAMY 204	<i>UTR</i> overexpression strain	<i>ura3</i> Δ:: <i>λimm434</i> / <i>ura3</i> Δ:: <i>λimm434</i> , <i>his1</i> Δ:: <i>hisG/HIS1</i> , <i>arg4</i> Δ:: <i>hisG/ARG4</i> <i>ADH1/ADH1/adh1</i> :: <i>P_{ADH1}</i> - <i>cartTA</i> :: <i>SAT1</i> , <i>RPS1/rps1</i> :: <i>Clp10</i> - <i>GTW- P_{TET}-UTR2</i>	This study

<i>pga31Δ</i>	<i>pga31Δ</i>	<i>ura3Δ::λimm434/ura3Δ::λimm434, arg4::hisG/arg4::hisG, his1::hisG/his1::hisG pga31::URA3/pga31::ARG4,</i>	(12)
CAM_K46	<i>PGA31</i> overexpression strain	<i>ura3Δ::λimm434/ura3Δ::λimm434, his1Δ::hisG/HIS1, arg4Δ::hisG/ARG4 ADH1/adh1::P_{ADH1}-cartTA::SAT1, RPS1/rps1::Clp10 -GTW- P_{TET}-PGA31</i>	This study

682 **Table 4. *C. albicans* strains used in this study**

683 **Phage display based isolation of CWP scFv binders from a human antibody library**

684 Solution phase biopanning and monoclonal phage binding enzyme-linked immunosorbent assay
685 (ELISA) were performed according to previously published methods (47). Briefly, a human
686 antibody library was subjected to repeated rounds of selection using biotinylated peptide antigens
687 corresponding to surface exposed regions of cell wall proteins Pga31 and Utr2. In the first
688 round, streptavidin magnetic beads (Dynabeads M280, Invitrogen) were coated with 500 nM of
689 biotinylated Utr2 or Pga31 peptide and phage particles displaying antibody fragments on their
690 surface were incubated for target binding. Phage particles bound to antigen-biotin complex were
691 eluted by triethylamine (TEA) and amplified by infecting *Escherichia coli* TG1 cells. For the
692 second and third rounds of panning, the coating concentration of biotinylated peptide antigen
693 was reduced to 100 nM and 10 nM respectively and rescued phage from previous rounds of
694 panning allowed to bind to the antigen for selection. For screening antigen specific phage
695 binders, 96-well plates (Nunc Maxisorp) were precoated with streptavidin to capture biotinylated
696 Pga31 or Utr2 peptides and monoclonal phage supernatant was added as described (48). Peptide
697 antigen binding ELISA was performed and individual phage monoclonals specifically binding to
698 CWP peptide antigen (and not recognising non-related biotinylated peptide) were selected for
699 antibody gene sequencing.

700 **Expression of soluble Pga31 and Utr2 antibody fragments (scAbs) in a bacterial system**

701 Positive phage clones with unique VH and VL genes were converted into soluble single chain
702 antibodies (scAbs) by cloning their respective scFv gene (VH-linker-VL) into the bacterial
703 expression vector pIMS147 and transforming *E. coli* TG1 cells for periplasmic expression as
704 described (30). ScAbs expressed in the bacterial periplasm were released by adding osmotic
705 shock solution consisting of Tris-HCl-sucrose and EDTA followed by MgSO₄ and incubated on
706 ice, gently shaking for 15 min each. Recombinant scAbs were purified using immobilized metal
707 affinity chromatography (IMAC) columns via binding of hexa histidine tagged protein to
708 activated Ni-sepharose beads and elution using imidazole. Purified scAbs were dialysed against
709 PBS and quantified either by SDS-PAGE, where the intensities of protein bands were compared
710 (Image J), or by calculating final scAb concentrations by measuring the absorbance values at 280
711 nm using Ultraspec 6300 pro UV/Visible spectrophotometer (Amersham, Biosciences).

712 **Reformatting CWP scAbs into human-mouse chimeric mAbs**

713 Utr2 and Pga31 scAbs were reformatted into human-mouse (IgG2a) chimeric mAbs by inserting
714 the antibody VH and V κ genes into a dual plasmid eukaryotic vector system encoding constant
715 heavy and light chain genes of mouse IgG2a isotype. VH and V κ genes of shortlisted scAbs
716 were custom synthesised by introducing the restriction sites BssHII and BstEII (for VH gene)
717 and BssHII and XhoI (for V κ gene) at their 5' and 3' ends respectively (GeneArt custom gene
718 synthesis service by Thermofisher), cloned into respective eukaryotic expression vectors
719 pEEDM2a (encoding mouse IgG2a constant regions) or pEEDM κ (for mouse κ constant domain)
720 using standard restriction enzyme digestion and ligation steps. Ligated DNA was purified using
721 ethanol precipitation and used to transform electrocompetent *E. coli* TG1 cells for plasmid
722 propagation.

723 **Production of Pga31 and Utr2 mAbs in a mammalian expression system**

724 For laboratory scale expression of mAbs, plasmids bearing chimeric antibody heavy and light
725 chain genes were prepared (EndoFree Plasmid Mega prep Kit, QIAGEN) and transfected into
726 Human Embryonic Kidney cells (HEK293F) (Life Technologies) using polyethylenimine (PEI).
727 Transfections were carried out using 1 mg of total DNA (500 µg each of VH and Vκ plasmid
728 DNA) and 1 l of cultured HEK293-F cell suspension maintained in sterile Freestyle 293
729 expression medium (Invitrogen) without antibiotics at 37 °C, with 8% CO₂, 125 rpm shaking.
730 The transfected cells were grown for 8 days and purified using ProSep A beads (Millipore) and
731 Econo-Pac chromatography columns (Biorad). Recombinant mAbs were eluted in 100 mM
732 glycine (pH 3.0) before neutralisation with 1 M Tris-HCl (pH 8.0). Purified mAbs were
733 quantified by SDS PAGE and A280 nm measurements.

734 **CWP Peptide, *C. albicans* cell lysate, and whole cell ELISA**

735 For ELISA using Pga31 or Utr2 peptides, 96 well Nunc Maxisorp plates were pre-coated with
736 100 nM streptavidin and blocked with 2% Marvel in PBS before adding 500 nM biotinylated
737 peptides. ScAb or mAb samples were incubated with the antigen in doubling dilutions and the
738 binding was detected using anti-Human C Kappa horseradish peroxidase (HRP) conjugated
739 secondary antibody (Sigma) (for scAbs) or anti-Mouse IgG (H+L) HRP secondary antibody
740 (Thermo Scientific) (for human-mouse chimeric mAbs).

741 For whole yeast cell or total cell lysate ELISA using wt, *pga31Δ*, *crh11/crh12/utr2Δ* and *PGA31*
742 overexpression strains of *C. albicans*, overnight cultures were inoculated into fresh YPD medium
743 with a starting OD_{600 nm} per ml of 0.1-0.2, grown at 30 °C until OD_{600 nm} per ml = 0.5-0.6 was
744 reached, then caspofungin (0.032 µg/ml) was added for 90 min.

745 For total cell lysate preparation, caspofungin treated or non-treated cells were harvested and
746 centrifuged for 5 min at 4000 rpm, washed with sterile dH₂O and 10 mM Tris-HCl pH 7.5 before
747 resuspending again in fresh Tris-HCl. Glass beads (0.5 mm diameter) were added (0.5 g to each
748 100 mg pellet) along with protease inhibitor solution (complete mini EDTA-free protease
749 inhibitor cocktail, Roche), dH₂O and 1 mM phenylmethylsulfonyl fluoride (PMSF) in ethanol.
750 Samples were subjected to 15 rounds of bead beating for 35 sec at speed 6.5 using a Fast Prep[®]-
751 24 instrument (MP Biomedicals, UK) with tubes placed on ice for at least 5 min in between each
752 round of bead beating. After centrifugation at 3000 rpm for 1 min to pellet the beads, the broken
753 cells suspension was transferred to sterile cold tubes. Cell lysate preparation was used to coat
754 ELISA plates as before.

755 For ELISA using *Candida* hyphae, cells were grown in RPMI-1640 medium (for 2-4 h) and
756 added to the wells for incubation at 37 °C for 1 h. For whole cell binding ELISA, *Candida*
757 coated wells were washed and blocked with 2% BSA (Sigma), followed by the addition of
758 double diluted scAb or mAb samples. Binding was detected using anti-Human C Kappa HRP or
759 anti-Mouse IgG (H+L) HRP and the resulting immunoreaction was measured as described
760 previously.

761 **Immunofluorescence imaging of antibodies binding to fungal cells**

762 Fungal cultures, grown as described above, were diluted 1:1000 in milliQ water and left to
763 adhere on a poly-L-lysine glass slide (Thermo Scientific, Menzel-Gläser) for 1 h. Cells were
764 washed three times in Dulbecco's phosphate-buffered saline (DPBS) and fixed with 4%
765 paraformaldehyde at room temperature. Blocking was done using 1.5% BSA which was
766 followed by washing and cell staining using mAbs at 25 µg/ml for 1 h at room temperature.
767 Alexa Fluor[®] 488 goat anti-mouse IgG antibody (Life Technologies) at 1 in 1000 dilution was

768 added to the slide for 1 h at room temperature and washed prior to staining with 25 µg/ml
769 calcofluor white (CFW) to stain cell wall chitin. Mounting medium and a coverslip were added
770 before images were taken using an UltraVIEW® VoX spinning disk confocal microscope
771 (Perkin Elmer, Waltham, Mass, USA).

772 ***Ex vivo* Macrophage Interaction assay**

773 **Macrophage culture**

774 J774.1 mouse macrophage-like cells (ECACC, Salisbury, UK) were cultured in Dulbecco's
775 Modified Eagle Medium (DMEM, Thermo Fisher) supplemented with 200 U/ml
776 penicillin/streptomycin, 2 mM L-glutamine (Invitrogen), and 10% (v/v) heat-inactivated foetal
777 calf serum in tissue culture flasks at 37 °C with 5% CO₂.

778 For interaction assays, macrophages were seeded at a density of 1×10^5 cells per well of a glass
779 imaging dish (Ibidi) and incubated overnight at 37°C, 5% CO₂. Immediately before
780 phagocytosis experiments, supplemented DMEM was replaced with pre-warmed supplemented
781 CO₂-independent medium (Thermo Fisher) to ensure macrophages remained viable during the
782 analysis of *C. albicans* interactions.

783 ***C. albicans* preincubation with test antibodies**

784 Prior to phagocytosis assays, *C. albicans* SC5314 yeast cells (3×10^5 cells) were either untreated
785 or pre-coated with 50 µg/ml anti-Pga31, anti-Utr2 mAbs or a commercially sourced anti-
786 *Candida* mouse IgG2a monoclonal antibody (MA1-7009) (Fisher Scientific) in pre-warmed
787 supplemented CO₂-independent medium and incubated at 37 °C with gentle shaking for 40 min.

788 **Live cell video microscopy of phagocytosis assay**

789 Video microscopy experiments were performed using an UltraVIEW® VoX spinning disk
790 confocal microscope in a 37°C chamber, with images captured at 1 min intervals over a 2 h

791 period using a Nikon camera (Surrey, UK). Six different videos were recorded for each antibody
792 or control group from two biological replicates, and subsequent analysis was conducted using
793 Volocity 6.3 imaging analysis software (PerkinElmer).

794 At least 25 macrophages were selected at random from each video to determine phagocytic
795 activity. Measurements taken included: (a) time of engulfment, defined as time between
796 macrophage establishing cell-cell contact to complete engulfment of the *C. albicans* cell and (b)
797 the length of intracellular hyphae at two time points (60 and 90 min). Mean values of the length
798 of 25 intracellular hyphae for each time point were calculated. A Shapiro-Wilk test for normality
799 was used to determine the distribution of data where appropriate. Kruskal–Wallis test with
800 Dunn’s multiple comparisons test was used to determine statistical significance using GraphPad
801 Prism 5.

802 **Investigating the therapeutic efficacy of CWP mAbs in mouse disseminated candidiasis** 803 **model**

804 All animal experimentation was done in accordance with UK Home Office regulations and was
805 approved by both the UK Home Office and an institutional animal welfare and ethical review
806 committee (AWERB). Female BALB/c mice, 7-9 weeks old (Envigo, Huntingdon, UK) were
807 randomly assigned to groups of 6 for treatment and control. *C. albicans* inoculum was prepared
808 by growing strain SC5314 in NGY medium for 16 h, with shaking at 30°C. Cells were harvested
809 and washed with saline, counted by haemocytometer, and resuspended in saline to provide an
810 inoculum of approx. 2×10^4 CFU/g mouse body weight in 100 μ l. Mice were infected
811 intravenously, and the actual inoculum level determined by viable cell counts. Depending on the
812 study, the treatment dose of mAbs was either 12.5 mg/kg or 15 mg/kg per mouse in 150 μ l.
813 MAbs were administered as prophylaxis or treatment. In prophylactic studies, a single dose of

814 antibody was delivered 3 h prior to challenge with *Candida* inoculum followed by either single
815 mAb dosing 24 h post infection and double dosing 24 and 72 h post infection. For treatment
816 only group, two doses of mAb were administered 24 and 72 h post *Candida* challenge. The
817 comparator drug caspofungin was dosed at 1 mg/kg at 24 h and 72 h post-infection. Vehicle
818 only control followed the same dosing pattern of test mAbs.

819 Mice were monitored and weighed every day during the course of experiments and at the end of
820 study period, mice were culled by cervical dislocation and organs, including kidneys, spleen and
821 brain, were removed aseptically and used to determine fungal burdens by plating out organ
822 homogenates and counting colonies after 24 h growth at 30°C.

823 In survival studies, mice which lost more than 20% of their initial body weight and/or showed
824 signs of a progressive systemic infection were culled by cervical dislocation and their day of
825 death recorded as occurring on the following day.

826 **Statistical Analysis**

827 Statistical analyses of mouse survival data were carried out with IBM SPSS and GraphPad Prism
828 5 was used for rest of the data. For antibody binding curves, data points are expressed as mean \pm
829 SEM (n=2). For macrophage assay and fungal burden in mouse kidneys and other organs, results
830 are shown as mean \pm SD. When comparing two or more groups, a Kruskal–Wallis test with
831 Dunn’s multiple comparisons was performed to determine statistical significance, across all
832 groups, then between different groups when there was a difference across all groups. Mouse
833 survival estimates were compared by the Kaplan-Meier log-rank test.

834

835 **References and Notes:**

- 836 1. F. Bongomin, S. Gago, R. O. Oladele, D. W. Denning, Global and Multi-National Prevalence
837 of Fungal Diseases-Estimate Precision. *J. Fungi (Basel)*. **3**, 10.3390/jof3040057 (2017).
- 838 2. K. Kainz, M. A. Bauer, F. Madeo, D. Carmona-Gutierrez, Fungal infections in humans: the
839 silent crisis. *Microb. Cell*. **7**, 143-145 (2020).
- 840 3. A. F. Talento, M. Hoenigl, Fungal Infections Complicating COVID-19: With the Rain Comes
841 the Spores. *J. Fungi (Basel)*. **6**, 10.3390/jof6040279 (2020).
- 842 4. M. A. Ghannoum, L. B. Rice, Antifungal agents: mode of action, mechanisms of resistance,
843 and correlation of these mechanisms with bacterial resistance. *Clin. Microbiol. Rev.* **12**, 501-517
844 (1999).
- 845 5. A. Arastehfar, T. Gabaldon, R. Garcia-Rubio, J. D. Jenks, M. Hoenigl, H. J. F. Salzer, M. Ilkit,
846 C. Lass-Flörl, D. S. Perlin, Drug-Resistant Fungi: An Emerging Challenge Threatening Our
847 Limited Antifungal Armamentarium. *Antibiotics (Basel)*. **9**, 10.3390/antibiotics9120877 (2020).
- 848 6. P. G. Pappas, M. S. Lionakis, M. C. Arendrup, L. Ostrosky-Zeichner, B. J. Kullberg, Invasive
849 candidiasis. *Nat. Rev. Dis. Primers*. **4**, 18026 (2018).
- 850 7. S. R. Lockhart, K. A. Etienne, S. Vallabhaneni, J. Farooqi, A. Chowdhary, N. P. Govender, A.
851 L. Colombo, B. Calvo, C. A. Cuomo, C. A. Desjardins, E. L. Berkow, M. Castanheira, R. E.
852 Magobo, K. Jabeen, R. J. Asghar, J. F. Meis, B. Jackson, T. Chiller, A. P. Litvintseva,
853 Simultaneous Emergence of Multidrug-Resistant *Candida auris* on 3 Continents Confirmed by
854 Whole-Genome Sequencing and Epidemiological Analyses. *Clin. Infect. Dis.* **64**, 134-140
855 (2017).

- 856 8. N. A. R. Gow, J. P. Latge, C. A. Munro, The Fungal Cell Wall: Structure, Biosynthesis, and
857 Function. *Microbiol. Spectr.* **5**, 10.1128/microbiolspec.FUNK-0035 (2017).
- 858 9. R. T. Wheeler, G. R. Fink, A drug-sensitive genetic network masks fungi from the immune
859 system. *PLoS Pathog.* **2**, e35 (2006).
- 860 10. C. Ibe, C. A. Munro, Fungal Cell Wall Proteins and Signaling Pathways Form a
861 Cytoprotective Network to Combat Stresses *J. fungi (Basel, Switzerland)*. **7**, 739 (2021).
- 862 11. J. C. Kapteyn, R. C. Montijn, E. Vink, J. de la Cruz, A. Llobell, J. E. Douwes, H. Shimoi, P.
863 N. Lipke, F. M. Klis, Retention of *Saccharomyces cerevisiae* cell wall proteins through a
864 phosphodiester-linked beta-1,3-/beta-1,6-glucan heteropolymer. *Glycobiology*. **6**, 337-345
865 (1996).
- 866 12. A. Plaine, L. Walker, G. Da Costa, H. M. Mora-Montes, A. McKinnon, N. A. Gow, C.
867 Gaillardin, C. A. Munro, M. L. Richard, Functional analysis of *Candida albicans* GPI-anchored
868 proteins: roles in cell wall integrity and caspofungin sensitivity. *Fungal Genet. Biol.* **45**, 1404-
869 1414 (2008).
- 870 13. P. W. De Groot, K. J. Hellingwerf, F. M. Klis, Genome-wide identification of fungal GPI
871 proteins. *Yeast*. **20**, 781-796 (2003).
- 872 14. J. Ruiz-Herrera, M. V. Elorza, E. Valentin, R. Sentandreu, Molecular organization of the cell
873 wall of *Candida albicans* and its relation to pathogenicity. *FEMS Yeast Res.* **6**, 14-29 (2006).
- 874 15. S. Ulrich, F. Ebel, Monoclonal Antibodies as Tools to Combat Fungal Infections. *J. Fungi*
875 (*Basel*). **6**, 10.3390/jof6010022 (2020).

- 876 16. M. Y. Heredia, M. A. C. Ikeh, D. Gunasekaran, K. A. Conrad, S. Filimonava, D. H. Marotta,
877 C. J. Nobile, J. M. Rauceo, An expanded cell wall damage signaling network is comprised of the
878 transcription factors Rlm1 and Sko1 in *Candida albicans*. *PLoS Genet.* **16**, e1008908 (2020).
- 879 17. E. Cabib, V. Farkas, O. Kosik, N. Blanco, J. Arroyo, P. McPhie, Assembly of the yeast cell
880 wall. Crh1p and Crh2p act as transglycosylases in vivo and in vitro. *J. Biol. Chem.* **283**, 29859-
881 29872 (2008).
- 882 18. G. Pardini, P. W. De Groot, A. T. Coste, M. Karababa, F. M. Klis, C. G. de Koster, D.
883 Sanglard, The CRH family coding for cell wall glycosylphosphatidylinositol proteins with a
884 predicted transglycosidase domain affects cell wall organization and virulence of *Candida*
885 *albicans*. *J. Biol. Chem.* **281**, 40399-40411 (2006).
- 886 19. M. Karababa, E. Valentino, G. Pardini, A. T. Coste, J. Bille, D. Sanglard, CRZ1, a target of
887 the calcineurin pathway in *Candida albicans*. *Mol. Microbiol.* **59**, 1429-1451 (2006).
- 888 20. C. Alberti-Segui, A. J. Morales, H. Xing, M. M. Kessler, D. A. Willins, K. G. Weinstock, G.
889 Cottarel, K. Fechtel, B. Rogers, Identification of potential cell-surface proteins in *Candida*
890 *albicans* and investigation of the role of a putative cell-surface glycosidase in adhesion and
891 virulence. *Yeast.* **21**, 285-302 (2004).
- 892 21. H. Si, A. D. Hernday, M. P. Hirakawa, A. D. Johnson, R. J. Bennett, *Candida albicans* white
893 and opaque cells undergo distinct programs of filamentous growth. *PLoS Pathog.* **9**, e1003210
894 (2013).

- 895 22. L. A. Walker, C. A. Munro, Caspofungin Induced Cell Wall Changes of *Candida* Species
896 Influences Macrophage Interactions. *Front. Cell. Infect. Microbiol.* **10**, 164 (2020).
- 897 23. C. A. Munro, Transcriptional profiling of putative glycosylphosphatidylinositol anchored
898 protein genes in *Candida albicans*. *Unpublished raw data, University of Aberdeen.* (2010).
- 899 24. A. F. Labrijn, M. L. Janmaat, J. M. Reichert, Parren, P W H I, Bispecific antibodies: a
900 mechanistic review of the pipeline. *Nat. Rev. Drug Discov.* **18**, 585-608 (2019).
- 901 25. J. Z. Drago, S. Modi, S. Chandarlapaty, Unlocking the potential of antibody-drug conjugates
902 for cancer therapy. *Nat. Rev. Clin. Oncol.* **18**, 327-344 (2021).
- 903 26. J. H. Lee, E. C. Jang, Y. Han, Combination immunotherapy of MAb B6.1 with fluconazole
904 augments therapeutic effect to disseminated candidiasis. *Arch. Pharm. Res.* **34**, 399-405 (2011).
- 905 27. F. M. Rudkin, I. Raziunaite, H. Workman, S. Essono, R. Belmonte, D. M. MacCallum, E. M.
906 Johnson, L. M. Silva, A. S. Palma, T. Feizi, A. Jensen, L. P. Erwig, N. A. R. Gow, Single human
907 B cell-derived monoclonal anti-*Candida* antibodies enhance phagocytosis and protect against
908 disseminated candidiasis. *Nat. Commun.* **9**, 5288-018 (2018).
- 909 28. A. Antoran, L. Aparicio-Fernandez, A. Pellon, I. Buldain, L. Martin-Souto, A. Rementería,
910 M. A. Ghannoum, B. B. Fuchs, E. Mylonakis, F. L. Hernando, A. Ramirez-Garcia, The
911 monoclonal antibody Ca37, developed against *Candida albicans* alcohol dehydrogenase, inhibits
912 the yeast in vitro and in vivo. *Sci. Rep.* **10**, 9206-020 (2020).

- 913 29. B. Petersen, C. Lundegaard, T. N. Petersen, NetTurnP--neural network prediction of beta-
914 turns by use of evolutionary information and predicted protein sequence features. *PLoS One*. **5**,
915 e15079 (2010).
- 916 30. A. Hayhurst, W. J. Harris, Escherichia coli skp chaperone coexpression improves solubility
917 and phage display of single-chain antibody fragments. *Protein Expr. Purif.* **15**, 336-343 (1999).
- 918 31. E. Pelfrene, M. Mura, A. Cavaleiro Sanches, M. Cavaleri, Monoclonal antibodies as anti-
919 infective products: a promising future? *Clin. Microbiol. Infect.* **25**, 60-64 (2019).
- 920 32. C. Boniche, S. A. Rossi, B. Kischkel, F. V. Barbalho, A. N. D. Moura, J. D. Nosanchuk, L.
921 R. Travassos, C. P. Taborda, Immunotherapy against Systemic Fungal Infections Based on
922 Monoclonal Antibodies. *J. Fungi (Basel)*. **6**, 10.3390/jof6010031 (2020).
- 923 33. I. V. Ene, C. J. Heilmann, A. G. Sorgo, L. A. Walker, C. G. de Koster, C. A. Munro, F. M.
924 Klis, A. J. Brown, Carbon source-induced reprogramming of the cell wall proteome and
925 secretome modulates the adherence and drug resistance of the fungal pathogen *Candida*
926 *albicans*. *Proteomics*. **12**, 3164-3179 (2012).
- 927 34. C. J. Heilmann, A. G. Sorgo, S. Mohammadi, G. J. Sosinska, C. G. de Koster, S. Brul, L. J.
928 de Koning, F. M. Klis, Surface stress induces a conserved cell wall stress response in the
929 pathogenic fungus *Candida albicans*. *Eukaryot. Cell*. **12**, 254-264 (2013).
- 930 35. F. M. Klis, G. J. Sosinska, P. W. de Groot, S. Brul, Covalently linked cell wall proteins of
931 *Candida albicans* and their role in fitness and virulence. *FEMS Yeast Res.* **9**, 1013-1028 (2009).

- 932 36. S. Austermeier, L. Kasper, J. Westman, M. S. Gresnigt, I want to break free - macrophage
933 strategies to recognize and kill *Candida albicans*, and fungal counter-strategies to escape. *Curr.*
934 *Opin. Microbiol.* **58**, 15-23 (2020).
- 935 37. A. L. Matveev, V. B. Krylov, Y. A. Khlusevich, I. K. Baykov, D. V. Yashunsky, L. A.
936 Emelyanova, Y. E. Tsvetkov, A. A. Karelin, A. V. Bardashova, S. S. W. Wong, V. Amanianda,
937 J. P. Latge, N. V. Tikunova, N. E. Nifantiev, Novel mouse monoclonal antibodies specifically
938 recognizing beta-(1-->3)-D-glucan antigen. *PLoS One.* **14**, e0215535 (2019).
- 939 38. V. Duncan, D. Smith, L. Simpson, E. Lovie, L. Katvars, L. Berge, J. Robertson, S. Smith, C.
940 Munro, D. Mercer, D. O'Neil, Preliminary Characterisation of NP339, a Novel Polyarginine
941 Peptide with Broad Antifungal Activity. *Antimicrob. Agents Chemother.* (2021).
- 942 39. L. Di, Strategic approaches to optimizing peptide ADME properties. *AAPS J.* **17**, 134-143
943 (2015).
- 944 40. J. L. Lau, M. K. Dunn, Therapeutic peptides: Historical perspectives, current development
945 trends, and future directions. *Bioorg. Med. Chem.* **26**, 2700-2707 (2018).
- 946 41. R. J. Keizer, A. D. Huitema, J. H. Schellens, J. H. Beijnen, Clinical pharmacokinetics of
947 therapeutic monoclonal antibodies. *Clin. Pharmacokinet.* **49**, 493-507 (2010).
- 948 42. M. C. Arendrup, T. F. Patterson, Multidrug-Resistant *Candida*: Epidemiology, Molecular
949 Mechanisms, and Treatment. *J. Infect. Dis.* **216**, S445-S451 (2017).
- 950 43. A. Safdar, J. Ma, F. Saliba, B. Dupont, J. R. Wingard, R. Y. Hachem, G. N. Mattiuzzi, P. H.
951 Chandrasekar, D. P. Kontoyiannis, K. V. Rolston, T. J. Walsh, R. E. Champlin, I. I. Raad, Drug-

952 induced nephrotoxicity caused by amphotericin B lipid complex and liposomal amphotericin B: a
953 review and meta-analysis. *Medicine (Baltimore)*. **89**, 236-244 (2010).

954 44. E. Albengres, H. Le Louet, J. P. Tillement, Systemic antifungal agents. Drug interactions of
955 clinical significance. *Drug Saf.* **18**, 83-97 (1998).

956 45. D. V. Zurawski, M. K. McLendon, Monoclonal Antibodies as an Antibacterial Approach
957 Against Bacterial Pathogens. *Antibiotics (Basel)*. **9**, 10.3390/antibiotics9040155 (2020).

958 46. A. M. Gillum, E. Y. Tsay, D. R. Kirsch, Isolation of the *Candida albicans* gene for orotidine-
959 5'-phosphate decarboxylase by complementation of *S. cerevisiae* *ura3* and *E. coli* *pyrF*
960 mutations. *Mol. Gen. Genet.* **198**, 179-182 (1984).

961 47. P. Chames, D. Baty, in *Antibody Engineering*, R. Kontermann and S. Dübel, Eds. (Springer
962 Berlin Heidelberg, Berlin, Heidelberg, 2010), pp. 151-164.

963 48. K. Charlton, W. J. Harris, A. J. Porter, The isolation of super-sensitive anti-hapten antibodies
964 from combinatorial antibody libraries derived from sheep. *Biosens. Bioelectron.* **16**, 639-646
965 (2001).

966 **Acknowledgments:** The authors gratefully acknowledge Kevin McKenzie and Lucy Wight
967 from the University of Aberdeen Microscopy and Histology Facility for training and access to
968 fluorescence microscopy and for their support & assistance in this work. The authors also
969 gratefully acknowledge Dr David Stead from Aberdeen Proteomics for his support & assistance
970 with the *Candida* proteome analysis and the staff of the University of Aberdeen Medical
971 Research Facility for their support & assistance with the mouse studies.

972 **Funding:** This work was supported by the following research grants:
973 High throughput and Fragment screening Fund, Scottish Universities Life Sciences Alliance
974 (SULSA)
975 Seed Corn Award from the University of Aberdeen Wellcome Trust Institutional Strategic
976 Support Fund
977 MRes Studentship by the Medical Research Council Centre for Medical Mycology at The
978 University of Aberdeen (grant number MR/P501955/1)
979 PhD studentship, Institute of Medical Sciences, University of Aberdeen
980 PhD studentship, Taibah University and Saudi Government Scholarship
981 PhD studentship by the European Union’s Horizon 2020 research and innovation program under
982 the Marie Skłodowska-Curie grant agreement no: H2020-MSCA-ITN-2014-642095 (OPATHY)
983 **Author contributions:** CAM, SP, AJP contributed to the concept and study design, CAM and
984 SP developed the methodology. SAA and LF performed recombinant antibody generation and
985 ELISAs, LF and MW completed IgG reformatting and production of mAbs for animal studies;
986 MM, THT and LAW performed ELISAs and IF staining; MM performed macrophage assays and
987 DM planned, conducted and analysed animal studies. CAM, SP, AJP contributed towards
988 funding acquisition and project administration and CAM, SP and LAW towards the supervision
989 and training of MRes and PhD students. SP wrote the original draft and CAM, DMM and AJP
990 completed review and editing. All authors had full access to the data and approved the
991 manuscript before it was submitted by the corresponding author
992 **Competing interests:** SP, AJP, CAM are inventors on a patent relating to development of
993 antifungal antibodies to surface exposed epitopes of fungal pathogens owned by the University
994 of Aberdeen. All the other authors declare that they have no competing interests.

995 **Data and materials availability:** All data are available in the main text or the supplementary
996 materials. Antibodies described in this paper will be available for research purposes through a
997 material transfer agreement with the University of Aberdeen

998
999

1000

1001

1002

1003

1004

1005 Supplementary Materials for

1006 **Monoclonal antibodies targeting surface exposed epitopes of *Candida albicans***

1007 **cell wall proteins confer *in vivo* protection in an infection model**

1008 Palliyil et al

1009 Corresponding authors: Soumya Palliyil, soumya.palliyil@abdn.ac.uk, Carol A Munro,

1010 c.a.munro@abdn.ac.uk

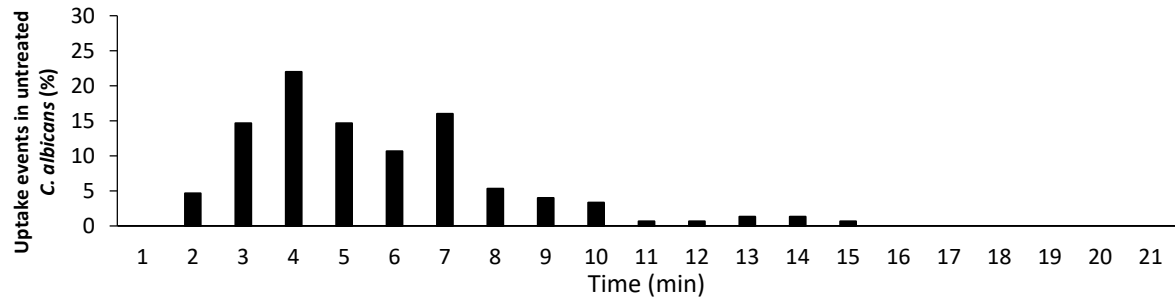
1011

1012 LIST OF SUPPLEMENTARY MATERIALS

1013 Figure S1

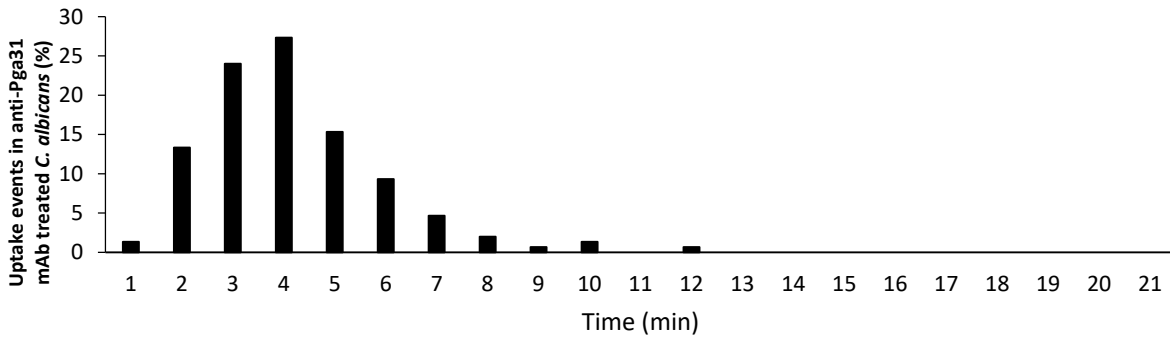
1014 Table S1

1015 A



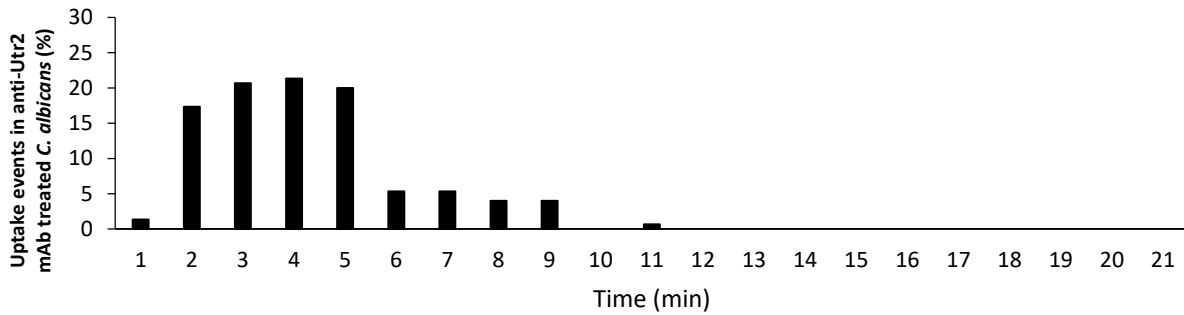
1016

1017 B

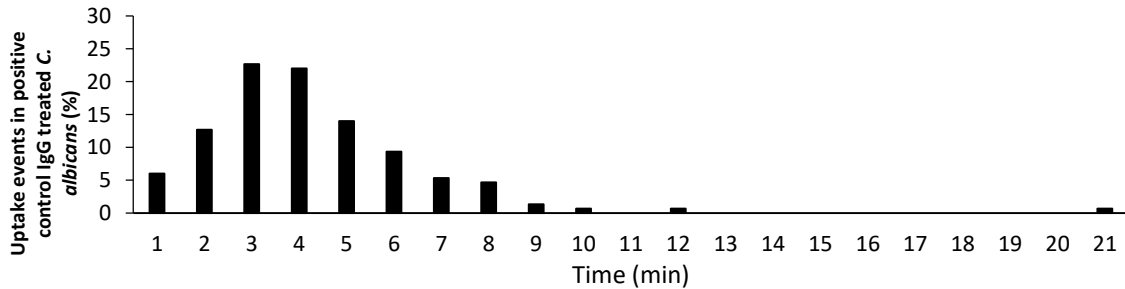


1018

1019 C



1020



1021 D

1022

1023 **Fig. S1. Engulfment of anti-Candida mAb treated *C. albicans* cells by mouse macrophages.**

1024 *The time taken for J774.1 macrophages to ingest live Candida cells following initial cell-cell*

1025 *contact verses the percentage of uptake events are plotted. (A) wt (B) Pga31 mAb (C) Utr2 mAb*
1026 *(D) positive control murine mAb. The rate of engulfment of all antibody-treated cells was faster*
1027 *than that of untreated C. albicans. Bars represent the percentages of uptake events (n = 6 videos*
1028 *for each antibody group from two biological replicates).*

1029

1030

Treatment group	Mean (\pm SD) change in body weight
Isotype Control	-13.77 \pm 3.00
Pga31 mAb	-9.49 \pm 2.56
Utr2 mAb	-10.79 \pm 1.80
Saline only	-11.59 \pm 2.89

1031

1032 ***Table S1. Average weight change in mice in study 1*** Groups of mice (n=6) were treated with
1033 *either Pga31 mAb (15 mg/kg), Utr2 mAb (15 mg/kg), mouse IgG2a isotype control (15 mg/kg) or*
1034 *saline, 3 h pre and 24 h post-infection in a murine model of disseminated candidiasis. Data*
1035 *represents mean change in body weight \pm SD (g) at day 2 compared with day 0 in mouse study 1.*

1036

1037